Inactivation of *Salmonella enterica* in 3D Printed Ready-to-eat Pudding

by

Yuliya Barsukova

A thesis submitted in partial fulfillment of the requirements for the degree of

Master of Science

in

Bioresource Technology

Department of Agricultural, Food and Nutritional Science

University of Alberta

Abstract

Three-dimensional (3D) food printing is a rapidly developing technology that transforms digital data as input to create a 3D edible physical product as output. It has the potential to change the food industry by offering highly customizable nutritional profiles and designs, while reducing food waste and the cost of manufacturing. The most widespread 3D printing method is extrusion-based, and it requires ingredients fluid enough to be extruded and viscous enough to hold their shape after deposition. As a result, many of these ingredients have high moisture content and some are meant to be consumed immediately after preparation as ready-to-eat products. Microbial food safety is an important consideration for these high moisture ready-to-eat 3D printed food products. Despite the technological advancements in 3D food printing, microbial safety aspect of 3D printed foods has not been fully investigated.

In this study, inactivation rate of *Salmonella enterica* serovar Typhimurium in a printed 3D square made of pudding was assessed. Before and during printing the pudding was heated at selected time-temperature combinations inside the 3D food printer. The temperature profiles evaluated were A (56.9°C), B (60.3°C), C (63.3°C) and D (66.7°C) and time increments were 10, 20, 30 and 40 min. Inactivation of *Salmonella* increased with temperature and heating time, with the highest reduction of >7 log CFU/g after 40 min at temperature profiles C and D. Inactivation of *Salmonella* after 10 min treatment at all the temperatures was not significantly different, and 40 min treatment at profile B was not significantly different from profiles C and D at 30 min. To preserve quality and nutritional parameters of 3D printed foods, lower temperature-longer time treatment may be preferred.

The second part of this study focused on the simulation of the heating of pudding in the plastic extrusion syringe inside the 3D printer by finite element modeling using axisymmetric 2D model. The experimental time-temperature relationships at the selected locations of the syringe

including at the center and the gap between the syringe and 3D printer's stainless-steel barrel during the heating of pudding were compared with simulation results. Overall, the predicted temperature changes were in good agreement with the experimental values. In addition, there was no considerable difference in the heating profiles of syringe quarter points, however, the contour plots showed heat loss due to convection at the top of the syringe. These results indicate the potential of finite element analysis to be used in conjunction with 3DFP as a useful tool for analyzing heat transfer and distribution in a closed system.

Acknowledgement

I would like to express my gratitude to Dr. John Wolodko and Dr. Roopesh Mohandas Syamaladevi for giving me the opportunity to pursue my Master's program under their supervision. I'm thankful for their guidance, patience, and immense support, especially during challenging times I've encountered while finishing my program. I also would like to thank Dr. Thava Vasanthan for agreeing to be an external examiner for my thesis defense and for investing his time in evaluating my thesis.

I would also like to thank my wonderful lab mates, namely, Harleen Kaur Dhaliwal, Amritha Jaya Prasad, Bina Gautam, Alvita Mathias, Abdullahi Adam, Barun Yadav, Samir Subedi, Ehsan Feizollahi, Dr. Basheer Iqdiam, Gaam Khemacheevakul, Anup Rana and Rodrigo Araya Olguin, for their assistance and fellowship.

Sincere thanks to Alberta Innovates for funding this study through Dr. Wolodko's Alberta Innovates Strategic Chair in Bio and Industrial Materials grant.

And lastly, I wouldn't be where I am today without my parents. Thank you, mom and dad, for everything you've done and keep doing for me.

Table of Contents

Chapter 1: Introduction and Objectives 1

1.1 Introduction 1

1.2 Hypothesis 2

1.3 Objectives 2

Chapter 2: Literature review 4

2.1 Introduction to 3D food printing 4

2.2 3D food printing operations and food materials 6

2.3 Microbial safety of 3D printed foods 8

2.4 Printing temperature 10

2.5 *Salmonella* spp. as pathogens of concern 12

2.6 Finite element analysis 13

Chapter 3: Materials and methods 15

3.1 Sample preparation for 3D printing 15

3.2 Measurement of water activity and moisture content 15

3.3 Bacterial strain and inoculum preparation 16

3.4 Design selection and creation 17

3.5 3D printing process 18

3.6 Selection of temperature for thermal treatment during to 3D printing 21

3.7 *Salmonella* recovery and enumeration 22

3.8 D_v and Z_v value determination 23

3.9 3D printer cylinder cross-section measurements 23

3.10 Temperature measurements 24

3.11 Finite element model creation 27

3.12 Statistical analysis 30

Chapter 4: *Salmonella* inactivation results and discussion 31

4.1 Effect of time-temperature combinations on inactivation of *Salmonella* 31

4.2 D_v and Z_v values 36

Chapter 5: Finite element analysis results and discussion 42

5.1 Experimental time-temperature measurements 42

5.2 Finite element analysis generated time-temperature graphs 44

5.3 Contour plots 47

Chapter 6: Conclusions and recommendations 50

6.1 Summary of key findings 50

6.2 Recommendations for future research 51

References 53

List of Tables

Table 1. Time and temperature parameters used in 3D food printing. 22

Table 2. Interior and exterior temperature measurements taken for each temperature profile. 25

Table 3. Thermo-physical properties used in the finite element model to predict heat transfer... 29

Table 4. Log reductions in Salmonella population influenced by combinations of temperature profiles A (55/56.9°C), B (58/60.3°C), C (61/63.3°C) and D (64/66.7°C) and time (10 min, 20 min, 30 min and 40 min). Data is the means of 3 independent experiments ± standard deviations. Below detection limit (BDL) indicates >7 reductions in Salmonella population. 34

Table 5. D_v values, slope and R^2 obtained from linear regression for Salmonella enterica inoculated into pudding at temperature profiles A (55/56.9°C), B (58/60.3°C), C (61/63.3°C) and D (64/66.7°C). 37

Table 6. Experimentally measured midpoint temperature of pudding in a syringe for temperature profiles A (55/56.9°C), B (58/60.3°C), C (61/63.3°C) and D (64/66.7°C) at 10 min, 20 min, 30 min and 40 min increments. Data are the means of 3 independent results ± standard deviations.43

List of Figures

Figure 1. Comparison of heat transfer in conventional canning and 3D food printing processes. 11

Figure 2. Flow diagram of a general 3D food printing process protocol. 18

Figure 3. Diagram of FoodBot 3D food printer components. 19

Figure 4. Diagram of a 3D food printing process from product selection to printing used in this study. 20

Figure 5. Visual depiction of 3D food printer's stainless-steel barrel (with and without the syringe). 24

Figure 6. Diagram of temperature interior and exterior measurement points, as summarized in the legend below. 26

Figure 7. Effect of temperature profiles A (55/56.9°C), B (58/60.3°C), C (61/63.3°C) and D (64/66.7°C) and time (10 min, 20 min, 30 min and 40 min) combinations on Salmonella population. DL means detection limit (> 7 log reduction). Data is the means of 3 independent experiments. Means with different letters are significantly different ($p < 0.05$). 33

Figure 8. Linear regression plots of temperature profiles A (55/56.9°C), B (58/60.3°C), C (61/63.3°C) and D (64/66.7°C) for pudding during heating+3D printing. Come-up time lines indicate an average time to reach the set printer temperature. Data points are the means of 3 independent experiments for each temperature profile. 38

Figure 9. Z_v values (temperature increase required for 1 log reduction in D_v value of S. Typhimurium in pudding during heating + 3D printing) slope and R^2 value. 39

Figure 10. Comparison of the experimentally measured temperature profile B (58/60.3°C) at the top quarter, middle and bottom quarter points down the centerline of the syringe. 43

Figure 11. Time-temperature graphs comparing experimentally measured interior temperatures (pudding) and exterior temperatures (gap) with the FEA simulated temperature results for profiles A (55/56.9°C), B (58/60.3°C), C (61/63.3°C) and D (64/66.7°C). 45

Figure 12. Contour plots of the heating rate of the pudding in the syringe upper half over time increments of 30s, 5 min, 10 min, 20 min, 30 min, 40 min and 50 min for temperature profiles A (55/56.9°C), B (58/60.3°C), C (61/63.3°C) and D (64/66.7°C). 49

List of Abbreviations

3DFP	3D food printing
3DP	3D printing
BDL	Below detection limit
CFIA	Canadian Food Inspection Agency
CFU	Colony forming unit
FDA	The United States Food and Drug Administration
FEA	Finite element analysis
FEM	Finite element method
FP	Food printer (in this context, 3D food printer)
RTE	Ready-to-eat
TSA	Tryptic soy agar
TSB	Tryptic soy broth
YE	Yeast extract

Chapter 1: Introduction and Objectives

1.1 Introduction

Three dimensional (3D) food printing (3DFP), also known as food layered manufacture has been gaining momentum in the past couple of decades, starting with the development of the first-generation food printer concept by Nanotek Instruments, Inc. in 2001 (Lille et al., 2018; Sun et al., 2015) and a physical prototype of a multi-material open-source 3D printer Fab@Home in 2006 (Lipton et al., 2015; Liu et al., 2017). The 3D foof printer has facilitated the digitalization of food manufacturing, providing flexibility in terms of material use, cost, energy, and ease of operation, as well as offering an opportunity for gastronomic creativity (Baiano, 2022; Lille et al., 2018; Yang et al., 2017). It allows the use of traditional food materials, such as chocolate, dough, and meat purees, as well as novel, non-traditional food sources, such as insects, algae, and plant-based materials, to produce foods with complex and customized designs, new textures, personalized and enhanced nutritional value (Derossi et al., 2018; Liu et al., 2017; Wang et al., 2018; Yang et al., 2017). While there is a perception that 3DFP will replace traditional methods of food production, it is more likely that it will find its niche market as part of Industry 4.0 instead (Godoi et al., 2019; Jagtap et al., 2021).

Ensuring food safety is important for 3D printed products, especially those with high moisture contents and those which do not require pre- or post-processing, such as commercially made mashed potatoes, puddings, purees, etc. While the amount of research on physicochemical properties of various printable food products and optimization of 3DFP processes is growing, the food safety aspect remains relatively unexplored. The major food safety challenges of 3DFP are the contamination risk from printer components and food ingredients, lack of hygiene and sanitation guidelines, and selection of suitable material and lack of post-processing steps to

eliminate microbial contamination in certain applications. Further, printing conditions can influence the survival of microorganisms in the end-products. For example, the temperature of the product during printing and printing time will determine the microbial inactivation during the 3D printing process. Many available 3D food printers can heat the food products/ingredients before or during the printing process, which can result in microbial inactivation. Microorganisms are sensitive to temperature, and the printability and quality changes in food can also be affected by the product temperature and exposure time before and during 3DFP. Understanding the relationship between temperature, exposure time and microbial inactivation rate is important to establish optimal time-temperature combinations for safe high moisture 3D printed foods.

1.2 Hypothesis

The overall hypothesis of the study is that heating as a part of a 3D printing process will inactivate pathogenic microorganisms like *Salmonella* spp. and will help to ensure microbial safety of 3D printed foods. Exposure time and temperature will affect the rate of inactivation of *Salmonella* in 3D printed foods, and selection of suitable time-temperature combinations is important to ensure food safety without affecting the printability.

1.3 Objectives

The general objective of this study was to evaluate the effect of selected time-temperature combinations on microbial inactivation, for producing safe-to-consume 3D printed foods.
The specific objectives are to:

1. Determine the inactivation kinetics of *Salmonella* in a commercially available pudding sample, which was heated, and 3D printed at selected temperature and time combinations.

2. Model and predict the heating patterns of pudding in a syringe used in 3D food printing by finite element analysis.

Chapter 2: Literature review

2.1 Introduction to 3D food printing

The 3D printing technology (3DP) uses layer-by-layer deposition to create various structures and is known as additive manufacturing (Yang et al., 2017). While conventional manufacturing is based on subtractive manufacturing, to create a final product, the additive manufacturing puts materials together, generating little or no waste (Ye, 2023). The 3DP was initially used in 1980s for the development of physical prototypes of computer-generated 3D designs for large production runs and was known as Rapid Prototyping (Baiano, 2020). Currently, 3DP is used in the areas of automotive manufacturing, building construction, medicine, space, consumer goods, etc. (Zhang et al., 2021). The 3D food printing (3DFP) was introduced in 2001, when Nanotek Instruments Inc. reported a method for creating a 3D custom birthday cake (Baiano, 2020; Sun et al., 2015). The basic steps to obtain a 3D printed product include generating a 3D model, converting it into a G-code that can be read by a printer using a specialized software, inputting the G-code into a printer hardware, and manipulating printing parameters such as speed, platform position and, in some instances, temperature for printing. The 3DFP comprises several types: extrusion-based printing, selective laser sintering, inkjet printing and binder jetting (Kern et al., 2018; Liu et al., 2017). Extrusion is the most common 3DP method due to its affordability and ability to efficiently extrude fresh food materials as a paste through a nozzle at a controlled temperature. There are three different extrusion techniques commonly used in 3DP including screw-based extrusion, air pressure driven extrusion, and syringe-based extrusion (Liu et al., 2018; Mantihal et al., 2019). Screw-based extrusion utilizes a screw to mix the material moving along the nozzle from an inlet and it works best with materials that have low viscosity and mechanical strength (Baiano, 2020, Liu et al., 2018). Air pressure driven extrusion uses air

pressure to propel material through the nozzle and it works best with liquids or low viscosity materials (Baiano, 2020). Syringe-based extrusion utilizes compression of the material by a plunger through the syringe nozzle and works best with materials with high viscosity and mechanical strength (Baiano, 2020). While continuous nozzle feeding is achievable only with screw-based extrusion, syringe-based extrusion is the most suitable for construction of complex 3D designs (Baiano, 2020; Liu et al., 2018). Some extrusion-based food printers, such as FoodBot 3D Printer, also work with disposable syringes, somewhat eliminating food safety concerns when it comes to contamination of printing parts.

3DFP technologies provide an opportunity to customize products, explore different geometric designs, produce less material waste, and utilize low volume manufacturing. 3DFP allows for product customization for specific population groups like youth, elderly, and people with nutrient deficiencies. It also provides an opportunity to utilize low-value or not fit for sale products, such as overmature fruit and vegetables, meat cut-offs, meal leftovers, and seafood by-products (Baiano, 2020; Godoi et al., 2019). Current ready-to-eat (RTE) products lack nutritional value and are often high in additives and calories, which leads to health issues like obesity, diabetes, and heart disease (Sundarsingh et al., 2023). 3DFP provides an opportunity to accommodate a variety of nutritional needs while also alternative proteins such as plants, insects, or microbes (Sundarsingh et al., 2023; Yang et al., 2017). 3DFP also has a potential for utilization during space missions and can increase quality and diversity of foods available for astronauts during long missions, thus having a positive effect on astronauts mental and physical health (Enfield et al., 2023). 3DFP also provides a novel tool for culinary creativity and food design (Jagtap et al., 2021). Park et al. (2023) describes using 3DFP to produce restructured beef steak with different amounts of marbling to cater to consumer's preferences.

At this point in time, there is no universally available software specifically for 3D printing of food materials that provide the user with different food options having different physicochemical parameters. Hence, the available software used for conventional 3D printing of plastics is commonly used for current 3D food printing applications (Godoi et al., 2019). The modelling of 3DFP processes can also be challenging since operating parameters used in existing software may not include properties such as viscosity and extrudability which are important to ensure food printability (Godoi et al., 2019).

2.2 3D food printing operations and food materials

Similar to conventional printers which use ink to transform a digital representation of an image into a physical print, 3DFP uses edible materials such as food inks (Yang et al., 2017). To get a high-quality printed product, it is crucial to choose a suitable ink. These should be a homogeneous, free flowing, adhesive material with relatively low viscosity. The ink should produce a dimensionally stable product, that will not deform while the next layer is being deposited (Anukiruthika et al., 2020; Nijdam et al., 2021, Wang et al., 2018). The most commonly used inks include purees (Lipton et al., 2010; Martínez-Monzó et al., 2019), gels (Liu et al., 2018; Wang et al., 2018), doughs (Lipton et al., 2010; Zhang et al., 2018), milk and egg proteins (Liu et al., 2018; Liu et al., 2019), semi-hard cheese (Kern et al., 2018) and chocolate (Lanaro et al., 2017; Mantihal et al., 2019; Yang et al., 2017). Many of these products undergo pre- or post-processing, however, some RTE commercial products don't require additional steps during the 3DP process. Material selection can impact microbial safety of food products, as some food inks support bacterial growth more than others due to their physicochemical properties such as high moisture content. If microbial contamination occurs at any stage (i.e., during material selection, preparation or printing), food poisoning can become a risk.

While a number of publications have focused on printability of 3D printed foods, physicochemical properties are responsible for quality, shelf-life, and safety of end products (Zhang et al., 2022). Intrinsic factors that affect microbial growth include pH, water activity, and nutrient content. Extrinsic factors include temperature, oxygen availability and relative humidity. Water activity, pH, and temperature are the most crucial product and process factors determining the storage stability and safety of canned foods and other thermally processed foods. Water activity (a_w) is related to the stability and quality of foods (Barbosa-Cánovas, 2020). The minimum a_w for microbial growth is 0.6 while for bacterial pathogens like *Salmonella*, the optimum a_w range is 0.93-0.95 (Barbosa-Cánovas, 2020).

In terms of printability, food materials need to be homogenous and have low viscosity to flow through the syringe nozzle in an extrusion-based printer. The loading of the food materials in the syringe introduces the possibility of air trapped bubbles, which reduces the quality of the final printed product and poses the risk of contamination (Sun et al., 2018). Viscosity is also directly related to extrusion temperature as viscosity decreases with increase in temperature (Liu et al., 2017). Mantihal et al. (2019) measured the viscosity of pre-crystallized dark chocolate at a temperature range from 25 to 40 ^oC and noticed a rapid decrease in viscosity and subsequent increase in flowability due to melting fat components. Martínez-Monzó et al. (2019) studied the effect of various temperatures on the viscosity of three potato puree formulations and found that as the temperature was increased from 10 to 30^oC, the apparent viscosity of the samples decreased. In addition to printability, the final printed product needs to be stable as well as during storage (maintain its shape after material deposition and over time). The stability depends on material's thermo-rheological properties such as glass transition temperature, gel-sol

transition temperature, storage and loss modulus, gelation, and melting (Kern et al., 2018; Liu et al., 2017; Yang et al., 2017).

2.3 Microbial safety of 3D printed foods

Currently, there have been limited studies focused on the microbial food safety of 3D printed foods which presents a challenge to both consumer and regulatory agencies. Derossi et al. (2018) designed a snack formula for children made of fruit, vegetables, and milk, and assessed its printability. It was noted that microbial safety during storage needed to be investigated further since the snack was printed at room temperature and did not involve any post-processing steps. Severini et al. (2018) 3D printed a mixture of fruit and vegetables at different print speeds and flow rates, and investigated their microbiological attributes for 8 days at 5°C. The results showed a significant increase in psychrophilic and mesophilic bacterial counts and yeast right after printing. This suggests the requirement of microbial inactivation steps during printing and post-processing, or the use of sterile ingredients for 3DP. Muro-Fraguas et al. (2020) investigated how 3D printed kitchen tools and food contact containers can harbor *Pseudomonas aeruginosa, Escherichia coli and Listeria monocytogenes* biofilms, and assessed approaches to reduce biofilm formation via cold plasma treatments. They emphasized that the nature of 3DP itself (i.e., the deposition of materials in consecutive layers) could introduce colonization and reproduction of various microorganisms depending on the properties of the ingredients. Zhang et al. (2022) noted that proper sanitation and storage practices remain a major issue when it comes to commercialization of 3DFP, and that there is very limited data on microbiological safety of 3DFP in the current literature. Enfield et al. (2023) suggested that commercial 3DP must have cleaning-in-place and cleaning-out-of-place systems and must be assessed using hazard analysis with identifies critical control points to ensure the safety of 3DP produced foods.

The shelf life and safety of 3D printed foods can significantly hinder the implementation of 3DFP development in the global market of food manufacturing. Verma et al. (2022) emphasized the lack of any regulatory frameworks established by the United States Food and Drug Administration (FDA) when it comes to 3DFP applications including topics such as food safety, shelf-life, personnel, facilities, and allergen regulations. Safety of 3D printed foods will also depend on the specific 3D food printing processes and the design of a printer. In addition to material deposition pattern issues as mentioned earlier, the printing process sometimes involves heating the food material prior to printing and cooling post-printing which can result in undesired bacterial growth if contaminated food ingredients are used or due to any cross contamination from the printer (Baiano, 2020). Another consideration is the design of 3D food printers is its ability to be cleaned easily. The Canadian Food Inspection Agency (CFIA) (2014) states that food equipment should be "accessible for cleaning, sanitation, maintenance and inspection" and equipment food contact surfaces should be "smooth, non-corrosive, non-toxic, non-absorbent and be able to withstand repeated cleaning and sanitation". The majority of mass-produced 3DP nowadays use relatively inexpensive systems and contain various parts and components that are either single use (i.e., plastic syringes and tips meant to be loaded with food material and discarded right after printing) or are reusable but may be hard to reach or difficult to fully clean (such as a plunger). Ideally, a commercially used 3D food printer should be easy to take apart, made with food safe materials, have a stainless-steel extruder, dishwasher or autoclave safe syringes and nozzles, and have no cracks or inaccessible spaces (Sun et al., 2018).

2.4 Printing temperature

Room temperature extrusion is the most common method used in 3DP; however, this process has a high risk for microbial contamination, especially with no post-processing of 3D printed product (Kern et al., 2018). Sun et al. (2018) states that room temperature extrusion is used for products that are naturally flowable and easy to extrude, such as doughs, jams, peanut butter, purees, pastes etc. Extrusion at higher temperatures called “hot melt extrusion” is a method where solid food material is melted (usually at the nozzle tip) before being deposited. This technology is often used in chocolates and chocolate products due to their crystallization behavior.

Thermal treatment of foods during 3DFP resembles a canning process. Conventional canning aims to destroy pathogenic microorganisms, while striving to keep the nutrients and quality parameters of the food intact (McHugh and Thai, 2020). The target microorganism of canning processes is *Clostridium botulinum*, which is found in water, soil, fish and mammals all over the world, and produces a lethal toxin causing paralysis (Featherstone, 2015). Inactivation of *C. botulinum* toxins in canned products is achieved by a sterilization process in a retort at 121°C for several minutes. Different target microorganisms require different time and temperature combinations. The canning process targets the anaerobic *C. botulinum* spores in the cold spot of a can, which is the slowest heating area in a container that determines the rate of heat penetration. Similarly, thermal treatment of foods during 3DP can target inactivation of any aerobic bacterial pathogen at the cold spot of the syringe, which will enhance the microbial safety of the final printed product. Fig. 1 shows the heat transfer and heating kinetics at the cold spot of a syringe used in 3DFP, which is similar to the heat transfer and heating kinetics in a can or jar during thermal treatment. Both processes operate through heat transfer, mainly by conduction heat transfer inside the syringe or can. In canning, steam is used as the heating

medium through convection, while in 3DFP, an electrical heater inside the stainless-steel barrel is used to heat the food from the outside via conduction. A small gap between the barrel and the syringe allows for some convection as well. However, heating a food product at a high temperature may influence its final structure and quality parameters. Therefore, focusing on temperatures close to 60°C in this study will allow us to investigate the effect of heat generated inside the 3D printed food product on *S.* Typhimurium in a semi-solid, high a_w, printable food product such as pudding.

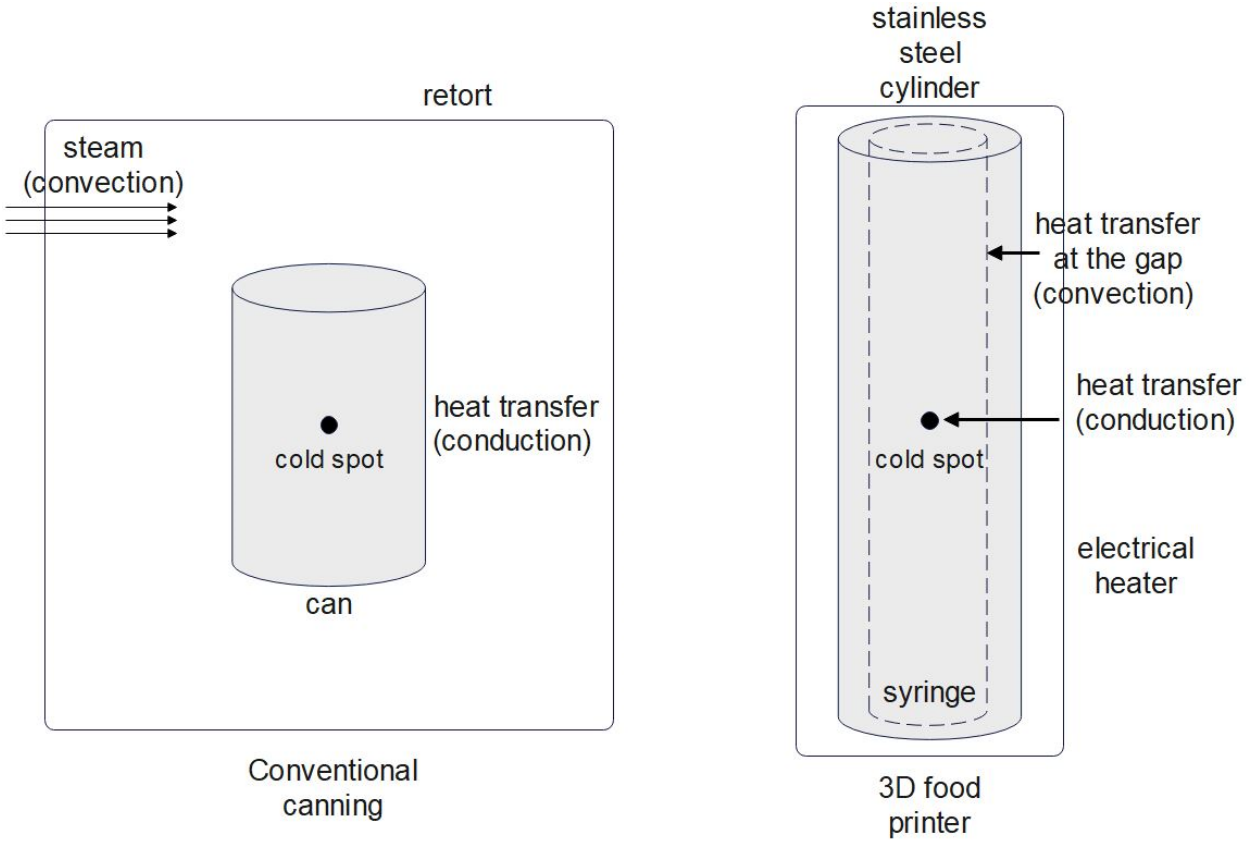

Figure 1. Comparison of heat transfer in conventional canning and 3D food printing processes.

2.5 *Salmonella* spp. as pathogens of concern

Many foodborne illnesses occur due to unhygienic practices, improper processing and an inadequate post-processing kill step, resulting in foodborne pathogen contamination (Sampson et al., 2023; Santos et al., 2008). *Salmonella enterica* is known for outbreaks related to a variety of commercially available products including peanut butter, poultry, eggs, ground beef, onions, and nuts (CDC, 2022; Ford et al., 2018; He et al., 2011; Morton et al., 2019). *Salmonella* spp. can be introduced from fresh and salt water, soil, and animal feces, and is spread via fecal-oral route (Featherstone, 2015; Sampson et al., 2023). Because salmonellosis requires as little as 15 cells for contamination, it is one of the most widespread foodborne infections worldwide and *S. enterica* is the most common cause of foodborne outbreaks in Canada (Featherstone, 2015; Korver and McMullen, 2017). *S. enterica* serovar Typhimurium has multiple virulent factors that assist in inducing disease in a host, including the ability to tolerate stomach acids, several pathogenicity islands, adhesins, flagella and biofilm formation elements (Fabrega and Vila, 2013). Its prevalence in our surroundings, virulent factors and ability to withstand food processing makes *Salmonella* spp. a major pathogen of concern in the food industry. Meat, specifically poultry harbor *Salmonella,* which results in outbreaks related to the consumption of internal organs and eggs (Korver and McMullen, 2017; Porto-Fett et al., 2019). Meat analogue products made from legumes like soy and peas, potatoes and fungi can also be contaminated with *Salmonella* due to improper processing (Sampson et al., 2023) Dairy products like cheese, egg-based products like pastries and in-shell pecans are also products of concern (Beuchat and Mann, 2010; Márquez-González et al., 2022; Moura-Alves et al., 2020). Antunović et al. (2018) successfully extracted *S*. Enteritidis from a variety of dairy products including pudding, yoghurt and cheese spread indicating that dairy products are a favorable environment Salmonella growth.

The abovementioned products have a relatively high moisture content and, paired with a possibility of *Salmonella* contamination introduced through the environment or processing, present a food safety challenge.

2.6 Finite element analysis

Finite element analysis (FEA) is a numerical modeling method for solving complex mathematical and engineering problems. FEA utilizes the finite element method (FEM) by dividing a larger object into smaller simplified sections (finite elements) and giving an approximate solution via simultaneous solving of algebraic equations. FEA was first utilized in the field of aerospace engineering for aircraft stress analysis, and is currently applied in various areas of engineering beyond solid mechanics (Bhavikatti, 2005). A basic FEA includes outlining the problem, making assumptions, defining materials and their properties, building a model, generating a mesh (finite elements), identifying boundary conditions, solving the problem, and reviewing the results (Madenci, 2015). FEA has been used in conjunction with conventional 3DP technology in various fields such as medicine (Ouldyerou et al., 2023), manufacturing (Mashhood et al., 2023), construction (Tahmasebinia et al., 2023), digital restoration (Papas et al., 2023) and, recently, food. Bareen et al. (2022) utilized FEA to assess printing variables such as ingredient concentrations, nozzle diameter, layer pattern and infill on textural characteristics of 3D printable formulations of RTE sweetmeats. The study demonstrated that modeling 3D designs before the printing process can improve printing accuracy, definition, and stability, resulting in high-quality personalized final printed products.

FEA has been applied to assess heat, moisture, and mass transfer in general food applications such as microwaving potatoes (Pandit and Prasad, 2003), ripening salami (Fabbri and Cevoli, 2015), microwave-infrared heating of zucchini (Yazicioglu et al., 2021), ohmic

heating of orange juice (Choi et al., 2020), potato chips drying (Kumar and Prakash, 2023) and freezing and thawing of meat and seafood (Fadiji et al., 2021). FEA can replace lengthy and costly experimentation by stimulating various scenarios and concepts in any environment (Fadiji et al., 2018). Heat transfer methods in food processing, such as microwave heating and canning, result in uneven distribution of temperature in food products (Pandit and Prasad, 2003). 3DFP is a similar process in terms of heat distribution and "cold spot" determination, as mentioned above, which also results in non-uniform heat absorption and transfer.

Chapter 3: Materials and methods

3.1 Sample preparation for 3D printing

The food product used in this study was Commercial Snack Pack™ brand vanilla pudding made with skim milk (Conagra Brands Canada Inc., Mississauga, Ontario) which was purchased locally. Each pudding pack consisted of 4 individual 99 g cups. One cup of vanilla pudding was used per experiment. Even though the pudding was shelf-stable, it was stored in a refrigerator at 4°C until usage. Prior to printing, it was taken out of the refrigerator the day prior to the experiment and left at room temperature to warm up in order to ensure easy and homogeneous blending.

3.2 Measurement of water activity and moisture content

Moisture content was determined by the oven drying method. Approximately 3 g of pudding was placed in a convection oven (Heratherm OGS60, Thermo Scientific, MA, USA) at 105 ^{o}C for 8 hours. The average moisture content on a wet basis (*MCw*) of two duplicate measurements was then calculated using the following equation:

$$MCw = \frac{m(H_2O)}{m(H_2O)+m_d} \quad [1]$$

where m (H_2O) = mass of sample with water removed and m_d = mass of dried sample.

Water activity of pudding was measured at room temperature using a water activity meter in triplicates (Model 4TE Dew Point Water Activity Meter, Decagon Devices, Pullman, WA). The water activity meter was calibrated before each measurement using water activity standards, such as 13.41 mol/kg LiCl (0.250 a_w) and 6.00 mol/kg NaCl (0.760 a_w).

3.3 Bacterial strain and inoculum preparation

S. enterica serovar Typhimurium (ATCC® 13311™) is a heat-sensitive strain that is greatly affected when heated to 60°C (Mercer et al., 2017). *Salmonella enterica* subsp. *enterica* serovar Typhimurium ATCC 13311 was obtained from -80°C glycerol stock culture stored in the Food Microbiology Lab (Agriculture Forestry Center, Edmonton, AB) and streaked on labeled Tryptic Soy Agar (TSAYE) plates with 0.6% yeast extract using an inoculation loop in order to be resuscitated to 10^9 CFU/mL. Incubated TSA plates were stored at 37°C for 24 h. After that, single colonies from the plates were transferred to 5 mL tryptic soy broth (TSB) with 0.6% yeast extract (TSBYE) and incubated in a shaking incubator at 37°C for 24 h, followed by sub-culturing with 100 µL inoculum and incubating again at 37°C for 18 h. After that 100 µL of broth culture was spread plated on TSAYE agar plates and incubated at 37 °C for 24 h. The next day, 2 mL of sterile 0.1% peptone water was added to each plate and the bacterial scraper was used to gather the lawn in a microcentrifuge tube. Cells were collected by centrifugation (Sorvall Legend Micro 21 Microcentrifuge, Thermo Fisher Scientific) at 10,000 RPM for 3 minutes, washed twice in 1 mL fresh sterile 0.1% peptone water, and resuspended in 1 mL of 0.1% peptone water for each microcentrifuge tube. Vortex mixer was used to homogenize the suspensions. The resulting *Salmonella* inoculum was mixed in a 15 mL Falcon tube. Overall, 6 mL of inoculum was prepared and serial dilution in a sterile 0.1% peptone water was performed, then plated on TSAYE and incubated at 37°C for 24 h. Out of 6 mL inoculum 3 mL was used to inoculate 99 g of pudding sample in a 400 mL beaker. The blend was vigorously stirred by hand for at least 1 minute with a stainless-steel spatula to ensure homogenous mixing and then covered with an aluminum foil and placed in a biosafety cabinet to avoid contamination. The mixing procedure was designed by incorporating food coloring (ClubHouse, McCormick Canada, London, Ontario) into the pudding sample until the color was homogenously distributed.

The results showed that homogenous mixing was achieved after at least 1 min of vigorous stirring by hand.

For each experiment, all the beakers, spatulas and tubes were sterilized for 1.5 hours at 121°C in an autoclave. All the syringes, tips and stoppers came individually wrapped in plastic, were used only once, and discarded after each experiment to avoid contamination of equipment and interference with the results.

3.4 Design selection and creation

Fig. 2 shows the steps involved in a general 3D food printing process. In order to create a printable design for this study, first, a three-dimensional structure in a stereolithography interface format file (.stl format) was created using the online 3D modeling program Tinkercad (Autodesk, Inc., California, USA). A simple 45 mm × 45 mm square was chosen for the design. The 3D model (.stl file) was then converted using "slicer" software into G-code which is a file format used directly by the 3D printers. This step was done using Cura 2.4 software (Ultimaker B.V., Geldermalsen, Netherlands), and the resulting G-code file was transferred to the 3D food printer using a flash drive.

The printed object was a 3D square (one layer) with actual dimensions of 42 mm × 43 mm. The print settings were 0.5 mm for the layer height, 50% fill density, 25 mm/s print speed, 40 mm/s retraction speed, 4.5 mm retraction distance, 30° support angle, 15% fill amount and 1 mm XY distance.

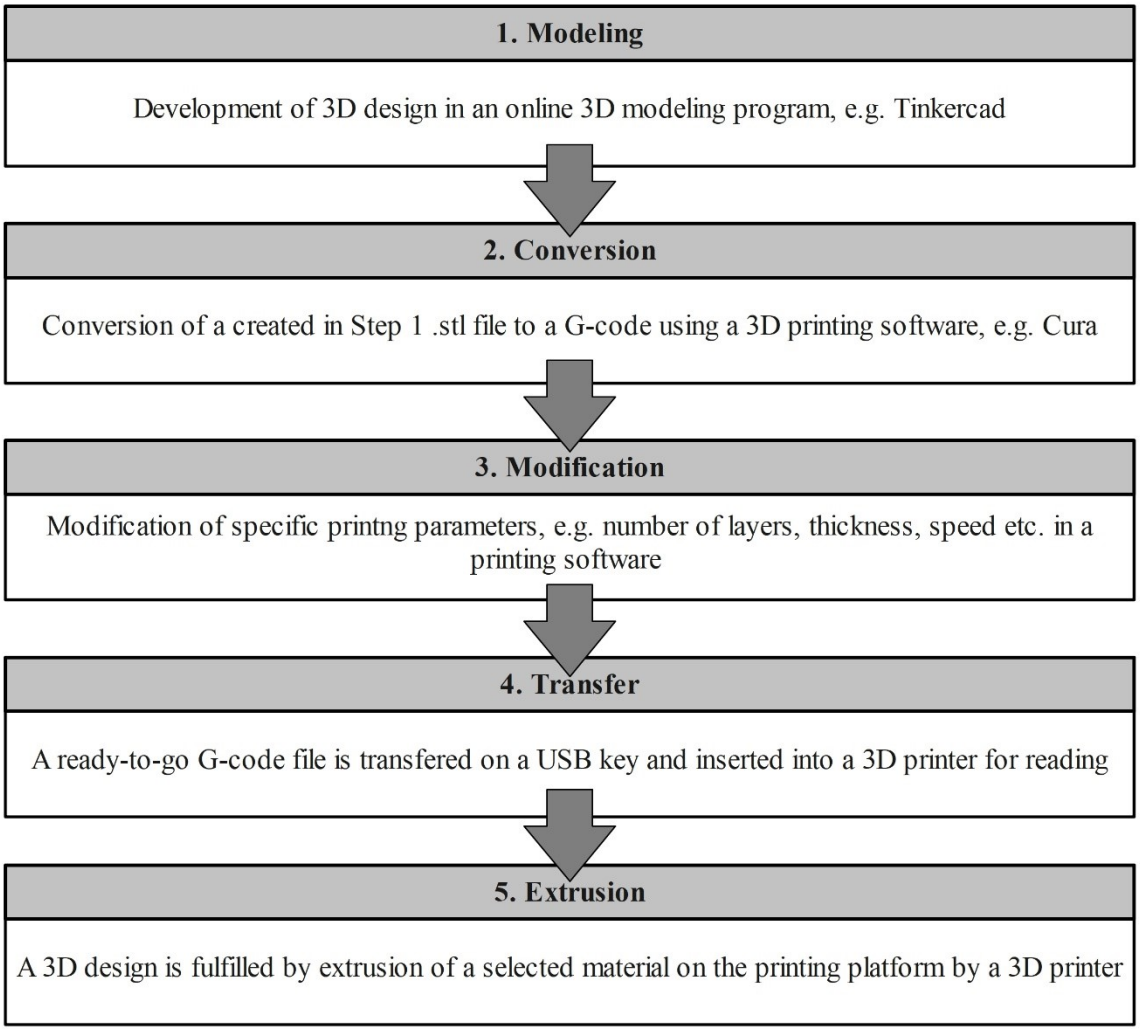

Figure 2. Flow diagram of a general 3D food printing process protocol.

3.5 3D printing process

The extrusion-based 3DP used in the study was a FoodBot 3D-printer (Shyin Tech., Hangzhou, China) as shown in Fig 3. The printer was equipped with a control screen, which allows the user to adjust the print settings, temperature, barrel, and platform positions, and to import the 3D model for extrusion from a USB key.

Figure 3. Diagram of FoodBot 3D food printer components.

The process of 3D food printing used in this study is outlined in Fig 4. First, the room temperature pudding was transferred in a 400 mL beaker using a stainless-steel spatula. Three milliliters of bacterial culture were added, and the mixture was stirred for at least 1 min. The mixture was then transferred into a disposable PipingPal 12’ pastry bag (DayMark Safety Systems, Bowling Green, OH). The disposable pastry bags were used to avoid air bubbles and ensure consistent printing. A plastic syringe was then filled with pudding, and some pudding was manually squeezed out of the filled syringe using a black default stopper to remove any initial air bubbles. A filled plastic syringe (14.1 cm in length and 2.35 cm in diameter) and a 0.84 mm nozzle was inserted into a stainless-steel chamber and pushed by a piston. An additional initial extrusion by the printer was performed to avoid over extrusion during printing.

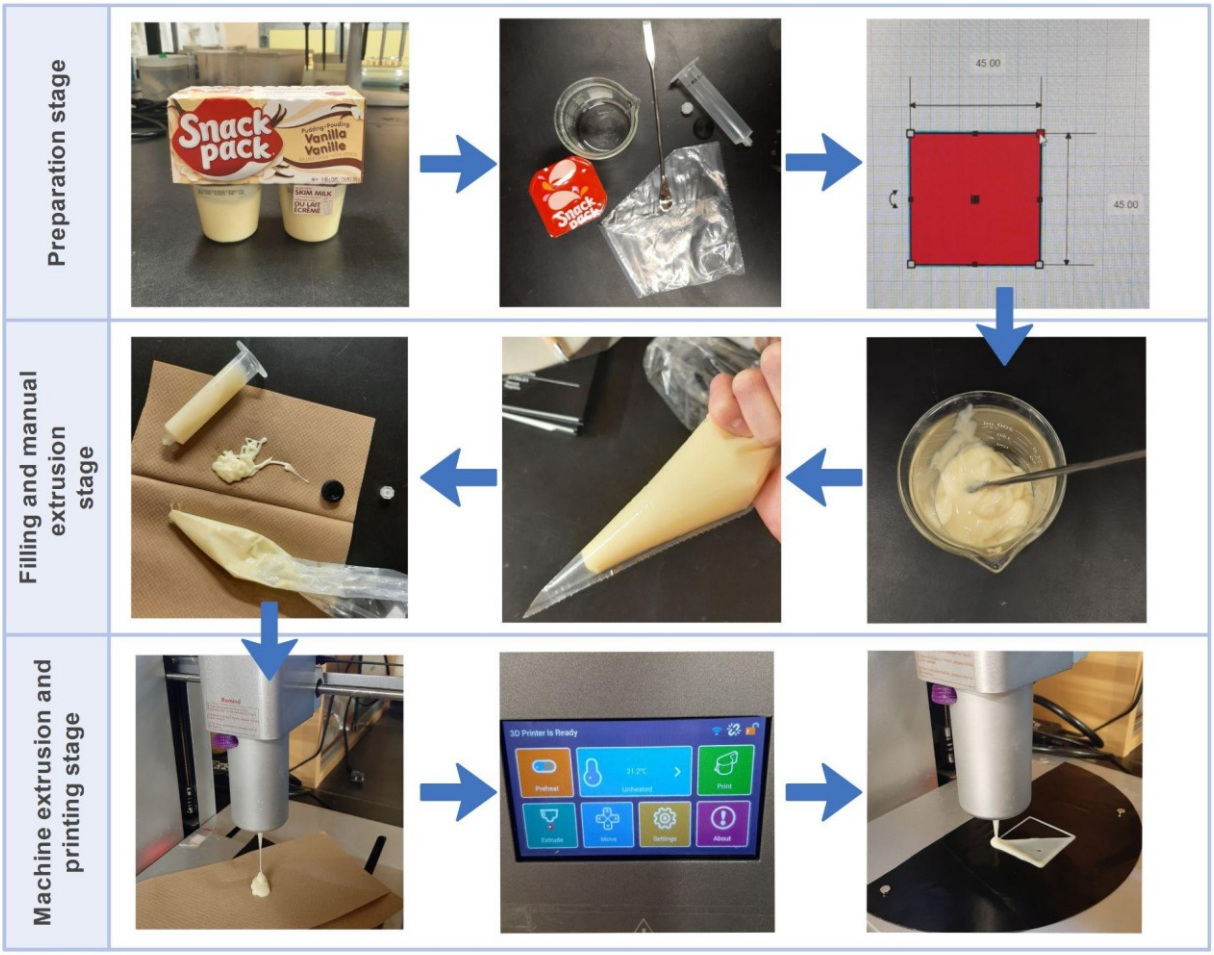

Figure 4. Diagram of a 3D food printing process from product selection to printing used in this study.

The average weight of the printed square was 1.7 g and average time to fully print it was 3 min. The weight and time fluctuated due to printer extrusion variations between each individual extrusion. All the mixing and transfer procedures were performed in a biosafety cabinet to avoid contamination. A Bunsen burner and 70% ethanol were used to sterilize the area near the weight scale for any procedures involving weight measurements.

3.6 Selection of temperature for thermal treatment during to 3D printing

The thermal treatment temperature profiles used in this study were determined by preliminary experiments. The setpoint temperature during 3DP set-up was shown to be approximately 2°C lower than the actual measured temperature. To reach the required (target) temperature, specific printer temperatures were chosen. For example, when the printer temperature was set at 55°C, the printer overshot and reached a stable temperature of 56.9°C. A stable temperature was determined by measuring come-up time at 30 second increments until the temperature reached a steady point for three consecutive values. Each printer temperature and actual reached temperature combination was assigned a letter designating a temperature profile, namely, A for 55/56.9°C, B for 58/60.3°C, C for 61/63.3°C and D for 64/66.7°C. For each temperature profile (A, B, C and D), a 3D square was printed at 4 different time periods: 10, 20, 30 and 40 min. The countdown started after the button "start heating" to the set printer temperature was pressed. For example, the printer temperature was set at 55°C, and once the button to initiate heating was pressed, the countdown to the first printing at 10 min was started. Subsequent samples were printed at the remaining time intervals (20, 30 and 40 min). The time required to print each square was approximately 2.5 min. The average come-up times to reach 55°C, 58°C, 61°C and 64°C were 24.4 min, 26.4 min, 25.8 min and 22.5 min, respectively. Table 1 summarizes time and temperature parameters during 3DFP used in this study.

Table 1. Time and temperature parameters used in 3D food printing.

Temperature profile	Temperature reached in the middle (°C)	Printer set point temperature (°C)	Time at which samples were printed (min)	Average come-up time (min)
A	56.9	55	10, 20, 30, 40	24.4
B	60.3	58	10, 20, 30, 40	26.4
C	63.3	61	10, 20, 30, 40	25.8
D	66.7	64	10, 20, 30, 40	22.5

3.7 *Salmonella* recovery and enumeration

The absence of *Salmonella* in the original pudding package (control) was confirmed by homogenizing 2 g of pudding sample in 6 ml of sterile 0.1% peptone water in a vortex mixer and plating on tryptic soy agar plates with 0.6% yeast extract. From a 400 mL beaker of pudding inoculated with 3 mL of inoculum, 4 g was added to two 15 mL Falcon tubes (2 g in each). 6 ml of sterile 0.1% peptone water was added to each tube and homogenized in a vortex mixer before plating on tryptic soy agar plates with 0.6% yeast extract by serial dilution. These inoculated, untreated pudding samples were used to calculate the inoculum counts before printing. After printing, each pudding sample (1 g) at every time and temperature combination was mixed with 100 mL sterile 0.1% peptone water. The homogenized suspension was transferred in a 15 mL labeled falcon tube. A serial dilution of the supernatant was conducted in sterile 0.1% peptone water, then plated on TSAYE in duplicate each and incubated at 37°C for 24 h. After a 24-hour incubation, *Salmonella* colonies were counted, and the results were expressed as log CFU/g. Logarithmic reductions were calculated by subtracting various temperature profiles and

treatment time combinations log counts from the average of inoculated, untreated pudding samples.

3.8 D_v and Z_v value determination

Decimal reduction time (D value) is the time at a constant specific temperature (isothermal conditions) required to reduce bacterial population by 1 log factor (Berk, 2008). Since the 3DFP process features non-isothermal conditions, true D-values cannot be calculated. Instead, this study used a subscript "v" to signify variable time and temperature conditions involved in 3DFP process. D_v represents the time for 1 log (90%) reduction to be achieved at non-isothermal conditions. Linear models of surviving bacterial population (Log CFU/g) versus time were created for each temperature profile, and the reciprocal of the slope of the generated curve was used to calculate D_v values. D_v values were determined using Excel linear regression analysis. The Z value is a thermal resistance constant, and it is the temperature increase required to reduce D value by 90% (Berk, 2008). Again, since the 3DFP process features non-isothermal conditions, the Z value was substituted by Z_v values which was determined by plotting each temperature and log of their corresponding calculated D_v values. The resulting linear regression line was used to obtain Z_v value by calculating the negative inverse of the slope.

3.9 3D printer cylinder cross-section measurements

The dimensions of the printer's stainless-steel barrel and the plastic syringe used to hold and dispense the pudding were measured and used as input for the FEA model in section 3.11. Fig. 5 shows the dimensions of the printer's components. The 3D stainless-steel heater barrel from the printer was 11.6 cm in length, and had an internal diameter of 2.5 cm and external diameter of 5.7 cm. The length of the plastic syringe was 11.5 cm without the tip and 14.1 cm with the tip. There was a slight gap of 0.15 cm between the stainless-steel cylinder and the

plastic syringe. A rubber stopper was placed inside the top of the syringe to assist extrusion via plunger motion from the 3DP.

Figure 5. Visual depiction of 3D food printer's stainless-steel barrel (with and without the syringe).

3.10 Temperature measurements

Prior to all experiments, the printer was placed in the biosafety cabinet to avoid room temperature fluctuations. According to the manufacturer, the heating source of the stainless-steel cylinder was a plastic heating film wrapped around for an even heat distribution.

The temperatures of the pudding inside the syringe were measured using an Omega HH25U thermometer and Type K thermocouple probe placed at three spots (as shown in Fig. 6): at the geometric center (midpoint of syringe), 1/2 from top to center and 1/2 from bottom to center. Only temperatures within the main body of the syringe were measured due to negligible

amount of pudding in the nozzle hub. Temperature data was recorded once the heating was imitated (i.e., when the "start heating" button was pressed), and was recorded every 30 s, starting from room temperature until it was stabilized (i.e., when three consecutive measurements of the same value were recorded). After that, the stabilized temperatures were measured every 30 s for 10 more min. The measurements were repeated in triplicate for each temperature profile (A, B, C and D) and location, with quarter-point measurements taken only for profile B, as shown in Table 2. In a separate set of experiments, the temperature at the gap was also measured by taping a thin wire thermocouple to the outside of the syringe in the same three spots as shown in Fig. 6 and placing the syringe inside the stainless-steel barrel. Temperature data recordings at the gap were taken at the same time intervals as the internal temperatures of syringe. Similar to the pudding temperature measurements, the measurements at the gap were repeated in triplicate for each temperature profile (A, B, C and D), with quarter-point measurements taken only for profile B, as shown in Table 2.

Table 2. Interior and exterior temperature measurements taken for each temperature profile.

Temperature profile	**Interior (pudding) measurements**			**Exterior (gap) measurements**		
	Center	Top	Bottom	Center	Top	Bottom
A	x			x		
B	x	x	x	x	x	x
C	x			x		
D	x			x		

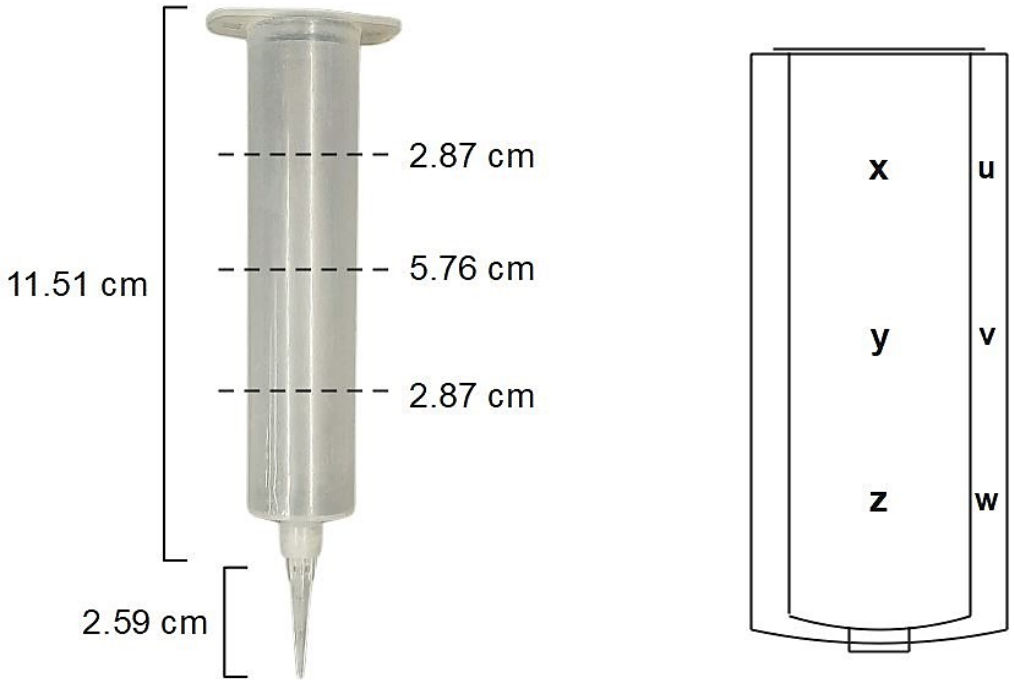

Figure 6. Diagram of temperature interior and exterior measurement points, as summarized in the legend below.

	Top Quarter	Center	Bottom Quarter
Interior Measurement Points (along axis of the syringe)	x	y	z
Exterior Measurement Points (gap between the barrel and syringe)	u	v	w

3.11 Finite element model creation

To supplement microbiological analysis of pudding inoculated with *S. enterica* and to demonstrate heating behavior of pudding in a cylinder, an FEA model of a plastic syringe containing pudding was developed. The temperature profiles generated by FEA were compared to temperature profiles obtained experimentally, and heat distribution was analyzed using Fourier's law of heat transfer rate for cylindrical geometries:

$$Q = \frac{2\pi\ K\ L\ (\Delta T)}{\ln\frac{r_o}{r_i}} \qquad [2]$$

where K = thermal conductivity, L = length, ΔT = temperature difference, r_o = outside radius, and r_i = inside radius

ANSYS Student 2023 R2 (Ansys Inc., Canonsburg, PA, USA) was used to create a 2D axisymmetric model of a plastic syringe filled with pudding. A transient thermal analysis system with a 2D analysis was selected. Engineering data included polypropylene type of plastic as syringe material (per manufacturer's declaration), with properties imported from ANSYS material database. No values for the thermophysical properties of pudding were directly found in the literature or online, so they were calculated by using established empirical formulas using the nutritional composition indicated on the label. Specific heat capacity and thermal conductivity of the pudding were determined using Equations 2 and 3, respectively, which are commonly used to estimate the properties of foods with known compositions (Berk, 2008; Singh and Heldman, 1984):

$$Cp = 1.424Mc + 1.549Mp + 1.675Mf + 0.837Ma + 4.187Mw \qquad [3]$$

$$K = 0.25Xc + 0.155Xp + 0.16Xf + 0.135Xa + 0.58Xw \qquad [4]$$

where X = is the mass fraction, and the subscripts are c = carbohydrate, p = protein, f = fat, a = ash, and w = water.

The density of the pudding sample was measured by water displacement method, where a 100 mL graduated cylinder was filled with 50 mL of water, and a known mass of pudding was added. The initial volume of water was subtracted from the volume displaced by the pudding, and the known mass of pudding was divided by that number to get the density of the sample. The measurement was repeated seven times. The abovementioned plastic syringe measurements were used to create a geometry of a syringe half in Design Modeler. The geometry was then imported into Ansys Mechanical where the rest of the analysis was conducted. Symmetry boundary conditions were added to geometry and the model was meshed. The actual measured temperatures over time at the syringe-barrel gap (see the preceding section) were used as the boundary conditions at the exterior of the syringe cylinder for the FEA model. The initial temperature was matched with the average measured room temperature for each individual temperature profile. A convection term was added at the top of the syringe to indicate some loss of heat through a rubber stopper. Total analysis time was selected to be 3000 s (50 min) with 30 s intervals to match experimental temperature measurements. The solution contained the average temperature distribution values, as well as middle and quarter points of the syringe. Table 3 summarizes the thermo-physical properties used in the FEA model and their sources.

Table 3. Thermo-physical properties used in the finite element model to predict heat transfer.

Parameter	Value	Units	Source
Pudding density	879 ± 0.04	kg/m^3	Measured by water displacement
Pudding thermal conductivity	0.499	W/m°C	Calculated from nutrition label (Berk, 2008; Singh and Heldman, 1984)
Pudding specific heat	6852.6	J/kg°C	Calculated from nutrition label (Singh and Heldman, 1984)
PP plastic density	903.4	kg/m^3	Ansys material database
PP plastic thermal conductivity	0.209	W/m°C	Ansys material database
PP plastic specific heat	1600	J/kg°C	Ansys material database
Mesh, element size	0.001	m	
Temperature, initial	-	-	Matched with initial experimental temperature for each temperature profile
Temperature, applied at the external plastic face	-	-	Temperature measured at the gap for each temperature profile
Convection term	-	-	Applied at the top of the syringe
Convection film coefficient	50	$W/m^2°C$	Ansys default value
Analysis time	3000	s	

3.12 Statistical analysis

The experiments were performed independently in triplicates. The statistical analysis was performed using SAS Studio 9.4 University Edition (Proc Glimmax, SAS Institute Inc., Cary, NC, USA). Tukey's LSD test ($p < 0.05$) to assess significant differences between means. A two-way analysis of variance ANOVA was used to evaluate the effects of both time and temperature on the pudding samples.

Chapter 4: *Salmonella* inactivation results and discussion

4.1 Effect of time-temperature combinations on inactivation of *Salmonella*

The main goal of food preservation and processing technologies is to ensure a maximum threshold of safety without compromising the product's physicochemical attributes like color and texture. Many of these technologies eliminate, inhibit the growth, or reduce the number of microorganisms to levels safe for consumption (Silva and Evelyn, 2023). Microbial inactivation is strongly dependent on the product's physicochemical characteristics, such as moisture content, number of ingredients and their individual characteristics, temperature and storage time, presence of preservatives, etc. Antunović et al. (2018) states that since milk is rich in nutrients, high in water content and has close to neutral pH, dairy products like pudding are an excellent medium to support growth of bacteria like *Salmonella* Enteritidis. Snack Pack™ pudding is a shelf-stable product with a measured moisture content of 77% and 0.996 ± 0.003 a_w, it is considered a good medium for *Salmonella* spp. inactivation.

The two-way ANOVA analysis revealed that time and temperature had a strong interaction between each other, and they both had an effect on resulting log reductions in *Salmonella* population. Fig. 7 demonstrates the results of time-temperature combinations on the survival of *Salmonella* population, with Table 4 providing log reduction numbers. The 10 min treatment was shown to be ineffective for all temperature profiles, with no log reductions across all experiments. The initial average microbial load was 10.30 CFU/g, 10.38 CFU/g, 10.32 CFU/g and 10.24 CFU/g for temperature profiles A, B, C and D, respectively. The microbial load increased slightly after 10 min for profiles A and C, indicating slight bacterial growth. The 10- and 20-min treatments for temperature profiles A and B had little influence on persistence of *Salmonella* in 3D food printed samples. The 20 min treatments in temperature profiles C and D

started showing a positive trend for bacterial inactivation due to an increase in temperature. A sharp contrast was observed between 20 and 30-min treatments in the temperature profile B, with an almost 3-log difference in reduction. Below detection limit (BDL) of 2.48 log CFU/g indicated that there was >7 log reduction in *Salmonella* population. BDL was observed in the 40 min treatments profiles C and D, which had the strongest effect on bacterial load and were significantly different from all other combinations. The 40 min treatments in temperature profiles C and D exhibited BDL log reductions, confirming that longer time and higher temperature combinations are the most effective treatments. From a food safety standpoint, a treatment time of 30 min or longer was required to reduce the *Salmonella* counts at lower temperatures, e.g., 56.9 to 60.3°C. According to data from the temperature profiles A and B, a 40 min treatment yielded a log reduction of 2.43 for A and a 30 min treatment yielded a higher reduction of 3.55 log for B. Higher temperatures of profiles C and D, namely 63.3-66.7°C require shorter treatment time of 20 min to achieve the same results. Temperature profile C had a similar reduction effect at 20 min compared to 40 min for profile A. The log reductions at 20 min for temperature profile D were comparable to that at 30 min for time-temperature profile B.

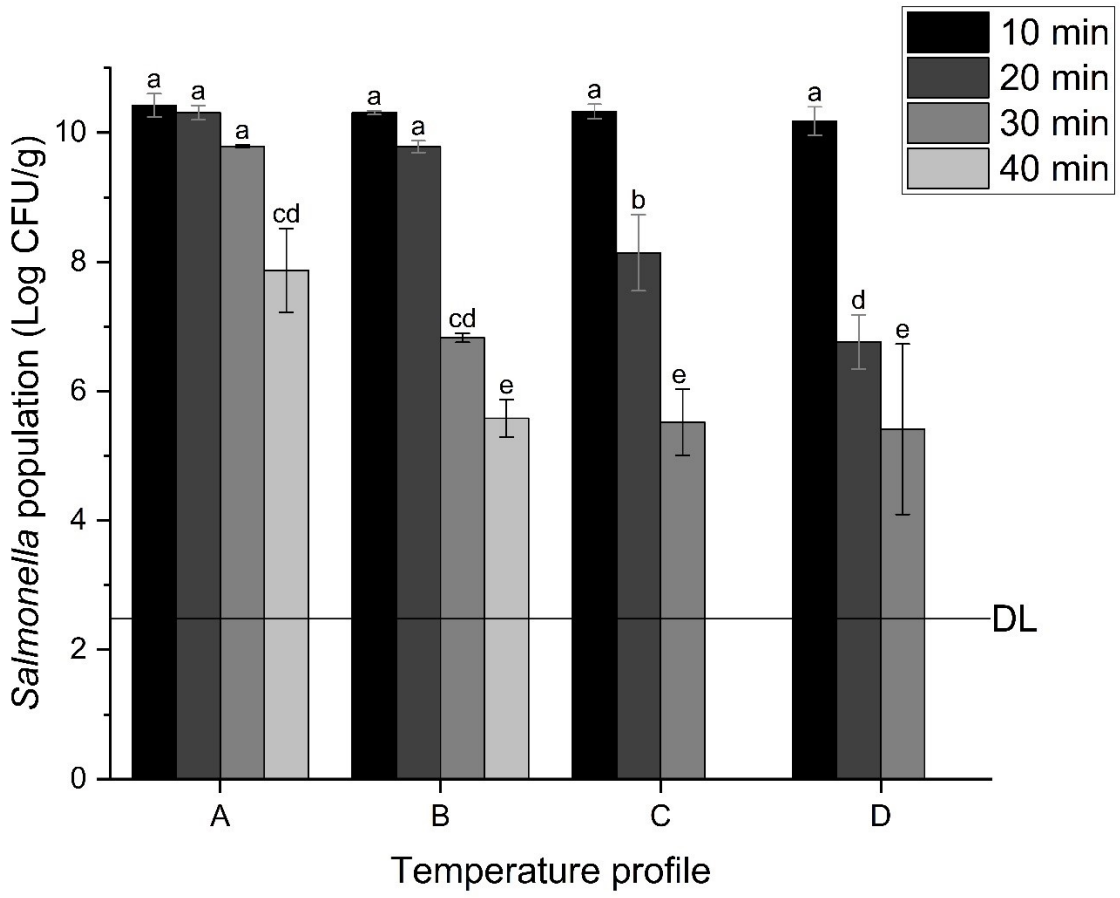

Figure 7. Effect of temperature profiles A (55/56.9°C), B (58/60.3°C), C (61/63.3°C) and D (64/66.7°C) and time (10 min, 20 min, 30 min and 40 min) combinations on *Salmonella* population. DL means detection limit (> 7 log reduction). Data is the means of 3 independent experiments. Means with different letters are significantly different ($p < 0.05$).

Table 4. Log reductions in *Salmonella* population influenced by combinations of temperature profiles A (55/56.9°C), B (58/60.3°C), C (61/63.3°C) and D (64/66.7°C) and time (10 min, 20 min, 30 min and 40 min). Data is the means of 3 independent experiments ± standard deviations. Below detection limit (BDL) indicates >7 reductions in *Salmonella* population.

Time (min)	*Salmonella* reduction (log CFU/g) corresponding to selected temperature profiles			
	A	B	C	D
10	-0.12 ± 0.17	0.07 ± 0.08	-0.01 ± 0.04	0.06 ± 0.22
20	-0.01 ± 0.07	0.60 ± 0.18	2.18 ± 0.71	3.47 ± 0.49
30	0.51 ± 0.04	3.55 ± 0.15	4.80 ± 0.57	4.82 ± 1.32
40	2.43 ± 0.70	4.80 ± 0.39	BDL (>7)	BDL (>7)

While it might be challenging to compare the results of this study with other publications due to differences in products' physicochemical characteristics and experimental conditions, other semi-solid foods as well as meat-based products with similar inactivation temperature ranges can be discussed. Porto-Fett et al. (2019) studied the effect of holding times (3 to 30 min) and target temperatures (60°C to 73.9°C) on *Salmonella* inactivation in chicken liver pate cooked in a water bath. Higher cooking temperatures and longer come-up times, as well as holding times ensured greater inactivation rates, ranging from 0.3 log CFU/g at 60°C to 4.9 log CFU/g at

71.1°C. When a water bath was stabilized at 1°C above each target temperature as opposed to being stabilized at 74.9°C, bacterial reductions showed an increase up to 2.6 log CFU/g due to longer come-up times. When pate was held for 3 to 30 min after being cooked to target temperature, there was also an increase in pathogen reduction. The results provide a valuable combination of treatment temperature and time options for delicate products like pate.

Dhaliwal et al. (2021) worked with the same strain of *S. enterica* serovar Typhimurium (ATCC® 13311™) wet inoculated in skim milk powder, equilibrated to a_w 0.33 and 0.75 and treated in thermal death time cells in a 70°C water bath. Samples were taken at 5-minute increments until 25 min. Snack Pack™ pudding also contains skim milk from concentrate in the list of ingredients. The bacterial load after thermal treatment was reduced by 0.04 log CFU/g in a_w 0.33 sample and 1.55 log CFU/g in a_w 0.75 sample. Higher a_w allowed for greater reduction in pathogen counts, and the study also indicated that S. Typhimurium is less heat resistant than other serovars used.

Hamilton and Gibson (2023) examined transfer rates of Tulane Virus, *Salmonella* Typhimirium and *Listeria monocytogenes* from the spot inoculated stainless-steel food ink capsule (syringe) to the extruded in a 3D food printer pure butter, a powdered sugar solution, a protein powder solution, and a mixture of all three. *Salmonella* recovered from printed foods ranged from 6.5 to 8 log CFU in sugar and butter, respectively, and 7.7 log CFU in the mixture. Hamilton and Gibson (2023) point out that surface-to-food transfer of pathogens is one of the most common causes of foodborne illnesses in consumer homes and food service establishments, therefore, further assessment of pathogen transfer and biofilm formation in 3DFP is needed.

4.2 D_v and Z_v values

Using the microbial population reduction data from the previous section, the D_v values for temperature profiles A, B, C and D were determined to be 18.18 min, 7.65 min, 4.88 min and 4.93 min, respectively (Table 5). At lower temperatures, microbial inactivation rate was less compared to higher temperatures. An increase of 6.4°C in the printer temperature in profile C resulted in a decrease in time for 1 log reduction from 18.9 to 4.88 min compared to profile A. This 13.3-minute difference is significant considering the stability of heat sensitive nutrients and quality characteristics of food. The R^2 value increased with increasing temperature, indicating that treatment time plays a bigger role at higher temperatures when it comes to reducing *Salmonella* population in a food sample (Fig. 9). At temperature profile A the R^2 value was 0.6556, meaning that other factors account for the variation in *Salmonella* population at lower temperatures, such as possible heat resistance at lower temperatures during treatment before the come-up time was reached. The D_v values of C and D were very similar, unlike the difference between D_v values of A and B, indicating that *Salmonella* was more heat sensitive at a lower temperature range, namely the 56.9-60.3°C range. Fig 8 shows a steep decline of the curve between 56.9°C and 60.3°C, and a relatively flat curve at 63.3°C and 66.7°C. It's important to note that an average come-up time for all temperature profiles (see Table 1) was 24.8 min, with B having the longest come-up time of 26.4 min and C having the shortest come-up time of 22.5 min. Since a sharp decrease in microbial population happened at 20 min for temperature profiles C and D, come-up time accounts for most of the inactivation at higher temperatures.

Table 5. D_v values, slope and R^2 obtained from linear regression for *Salmonella enterica* inoculated into pudding at temperature profiles A (55/56.9°C), B (58/60.3°C), C (61/63.3°C) and D (64/66.7°C).

Temperature profile	**Slope**	**D_v-value (min)**	**R^2**
A	-0.05 ± 0.0231	18.18	0.6556
B	-13.08 ± 0.0296	7.65	0.8669
C	-0.2049 ± 0.0337	4.88	0.9249
D	-0.2029 ± 0.0286	4.93	0.9437

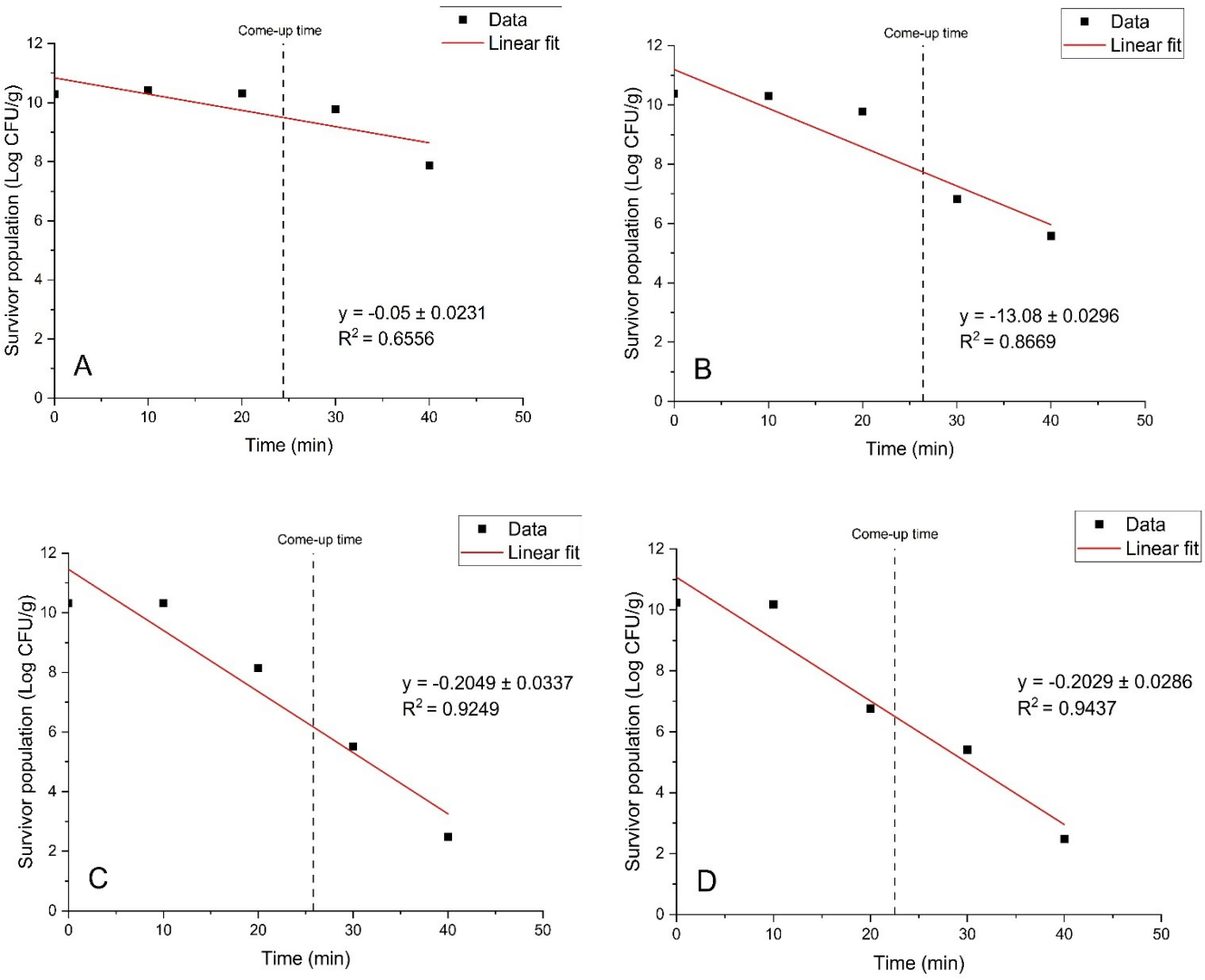

Figure 8. Linear regression plots of temperature profiles A (55/56.9°C), B (58/60.3°C), C (61/63.3°C) and D (64/66.7°C) for pudding during heating+3D printing. Come-up time lines indicate an average time to reach the set printer temperature. Data points are the means of 3 independent experiments for each temperature profile.

Since D_v values are based on non-isothermal conditions and are not true D values, the actual z-values could not be calculated. Instead, this study used a proxy Z_v value to define a thermal death time at non-isothermal variable conditions (Fig. 9). The Z_v value was determined as 17.09°C, which is the increase in treatment temperature (°C) to reduce the D_v value by 1 log.

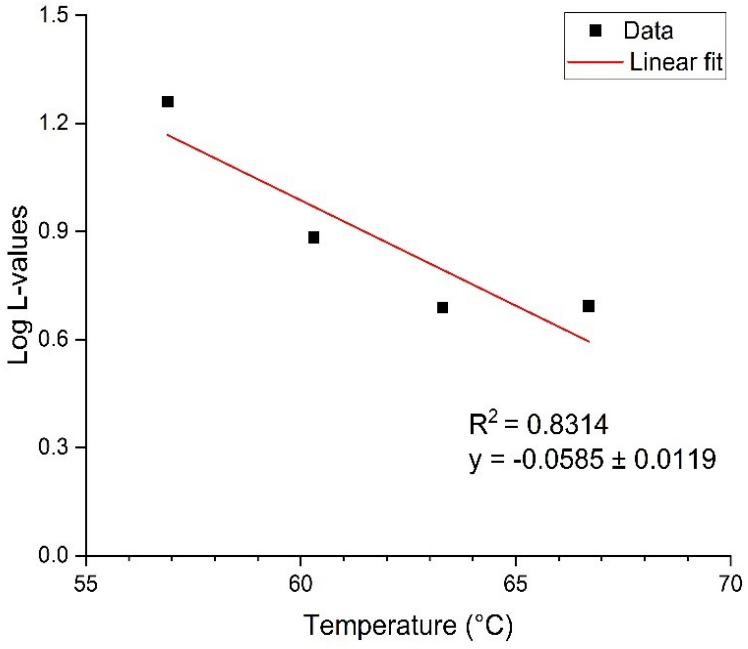

Figure 9. Z_v values (temperature increase required for 1 log reduction in D_v value of *S.* Typhimurium in pudding during heating + 3D printing) slope and R^2 value.

Márquez-González et al. (2022) investigated the effect of thermal treatment on the inactivation of *Salmonella enterica* in quesillo, a soft cheese made from raw milk. They used five different temperatures (48, 54, 60, 65, and 70°C) and specified time intervals for each individual temperature, ranging from 20 s at 70°C to 10 min at 48°C. The a_w of quesillo (0.980 ± 0.01) was similar to pudding used in this study (0.996 ± 0.003). The experimental conditions from Márquez-González et al. (2022) included a water bath and constant temperature; hence the reaction was isothermal and true D-values were calculated. The D-values were comparable to D_v values for profile A (55/56.9°C) and 54°C, with D_v and D values of 18.18 and 16.05 min, respectively. D-values for 54°C, 60°C and 65°C exhibited similar intervals to profiles A, B and C, with overall percentage decrease of 89.9% and 73.2% from the lowest to the higher temperature. Angelotti et al. (1961) evaluated the effects of 54-66°C treatments in custard on heat-resistant *Salmonella senftenberg* strain 775W and non-heat-resistant *Salmonella manhattan*. The D-values for *S.* senftenberg and S. *manhattan* at 60°C were 11.3 and 2.44 respectively, with z-values calculated to be 12.1 and 14.4. The D_v-value for temperature profile B (58/60.3°C) from this study fell between both ranges, being determined at 7.65. Angelotti et al. (1961) stated that determining thermal resistance using D-values is more flexible compared to F-value, because F-value heavily relies on bacterial concentrations being identical, while D-values allow comparison and extrapolation of data of various bacterial concentrations. The study also mentioned the term "lethality during lag" in the context of thermal death time tubes, meaning that bacterial inactivation happened during the time required for food to reach the target internal temperature. This is an important point to consider for future work in 3DFP thermal inactivation experiments, as inactivation might happen before the set temperature is attained, and it will result in poorer quality characteristics of a printed product.

Since microbial contamination is one of the biggest contributors to foodborne illnesses, it is important to consider some mitigation techniques related to 3DFP. Muro-Fraguas et al. (2020) showed that plasma-polymerized treatments can decrease the amount of biofilm production and bacterial attachment in 3D printed kitchen tools. This can also be applied to items involved in 3DFP like plastic syringes and rubber stoppers. Baiano (2020) also mentioned coating 3D printer's parts with food grade epoxy or resins to avoid bacterial growth in the cracks and inaccessible parts of the printer. In order to be considered food safe in an industrial setting, FP need to have a better design, critical control points system needs to be implemented and heating as a mitigation technique in 3DFP needs to be investigated further, encompassing a wider variety of pathogens and food products.

Chapter 5: Finite element analysis results and discussion

5.1 Experimental time-temperature measurements

There were no significant differences between the top quarter, middle and bottom quarter point of the syringe in the analyzed profile B, meaning the loss of heat through the rubber stopper or syringe nozzle tip was negligible to affect the heating rates of pudding. Fig. 10 showed that while the come-up temperature of the bottom quarter point slightly overshoots in the beginning and the top quarter point temperature slightly lags, they both match the middle point and exhibit lower reached temperatures towards the end. After 10 min of heating, the temperature for the top, middle and bottom points were 44.8°C, 45.2°C and 46.2°C, respectively, for the temperature profile B. Since the 44.8-46.2°C range did not influence the *Salmonella* population, there was no notable microbial inactivation at that time across all temperature profiles. Significant bacterial reduction of 3.55 log CFU/g for profile B started at a 30 min mark, with an average temperature of 58.5°C, increasing it to 4.80 log CFU/g at 59.4°C. Temperature profiles B, C and D display similar log reduction values of 4.80 log CFU/g at 40 min, 4.80 log CFU/g at 30 min and 4.82 log CFU/g at 30 min, respectively. These time increments correspond to 59.9°C, 62.1°C and 66.1°C, respectively (Table 6), suggesting that the same inactivation can be achieved at temperatures as low as 59.9°C for a shorter period of 30 min.

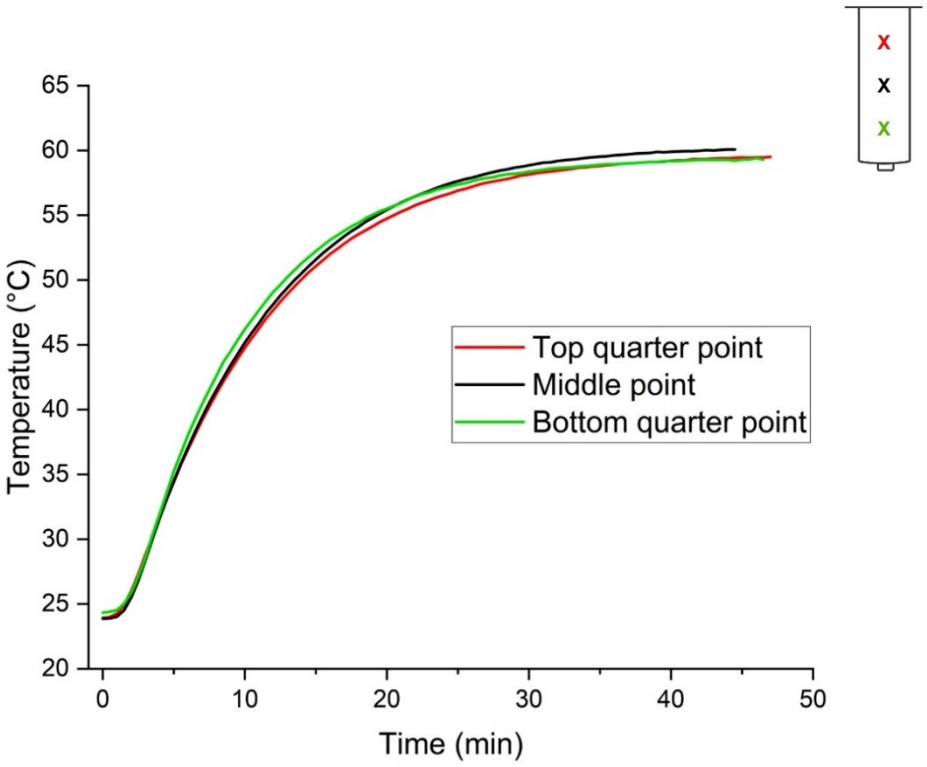

Figure 10. Comparison of the experimentally measured temperature profile B (58/60.3°C) at the top quarter, middle and bottom quarter points down the centerline of the syringe.

Table 6. Experimentally measured midpoint temperature of pudding in a syringe for temperature profiles A (55/56.9°C), B (58/60.3°C), C (61/63.3°C) and D (64/66.7°C) at 10 min, 20 min, 30 min and 40 min increments. Data are the means of 3 independent results ± standard deviations.

Time (min)	Reached middle temperature (°C)			
	A	B	C	D
10	44.2 ± 1.22	45.2 ± 1.49	47.7 ± 0.84	49.7 ± 1.17
20	53.4 ± 1.34	55.4 ± 0.54	58.5 ± 0.54	62.8 ± 1.42
30	56.1 ± 0.58	58.9 ± 0.42	62.1 ± 0.38	66.1 ± 0.72
40	56.7 ± 0.21	59.9 ± 0.34	63.2 ± 0.26	66.8 ± 0.38

5.2 Finite element analysis generated time-temperature graphs

The gap temperatures were measured to obtain the actual heat transfer temperature values at the outside of the syringe and were used as time-dependent boundary conditions for the finite element model. Fig. 12 shows the temperature comparison at the midpoint between the experimentally measured pudding in the syringe, FEA simulated temperature inside the pudding in the syringe, and experimentally obtained gap temperature between the plastic syringe and the printer barrel. The gap temperature data show the heating trend of the outside of the syringe due to the printer's electrical heater, with the rapid initial rise in temperature and a slower lagging curve afterwards. Profiles A and D had a slight dip in the curve when the printer overshot the temperature, namely, from 47.6°C to 47.3°C at 2 min for profile A and from 59.1°C to 58.7°C at 2.5 min for profile D. The heating rate continued in a smooth manner after that. Profiles B and C didn't have a dip, but a small lag instead, namely, 49.5°C at 2 and 2.5 min for profile B and from 49.2°C to 49.4°C at 2.5 min for profile C. Pudding temperature lines had a slight lag in the beginning but appeared continuously steady afterwards, until a relative plateau towards the end of the heating process.

FEA simulated temperature results were in good agreement with the experimentally obtained lines for all temperature profiles. The FEA models for profiles A and B overestimated the experimentally measured temperature slightly, while C and D were underestimated (with profile C showing the greatest difference). The highest deviation was 0.46 at 16 min mark for profile A, 0.48 at 4 min for profile B, 1.36 at 5.5 min for profile C and 0.67 at 9 min for profile C. There was a trend of increasing deviation before the come-up time was reached and decreasing deviation towards the end of the heating process. Differences between initial (room) temperature values at the start of each analysis might be accountable for that.

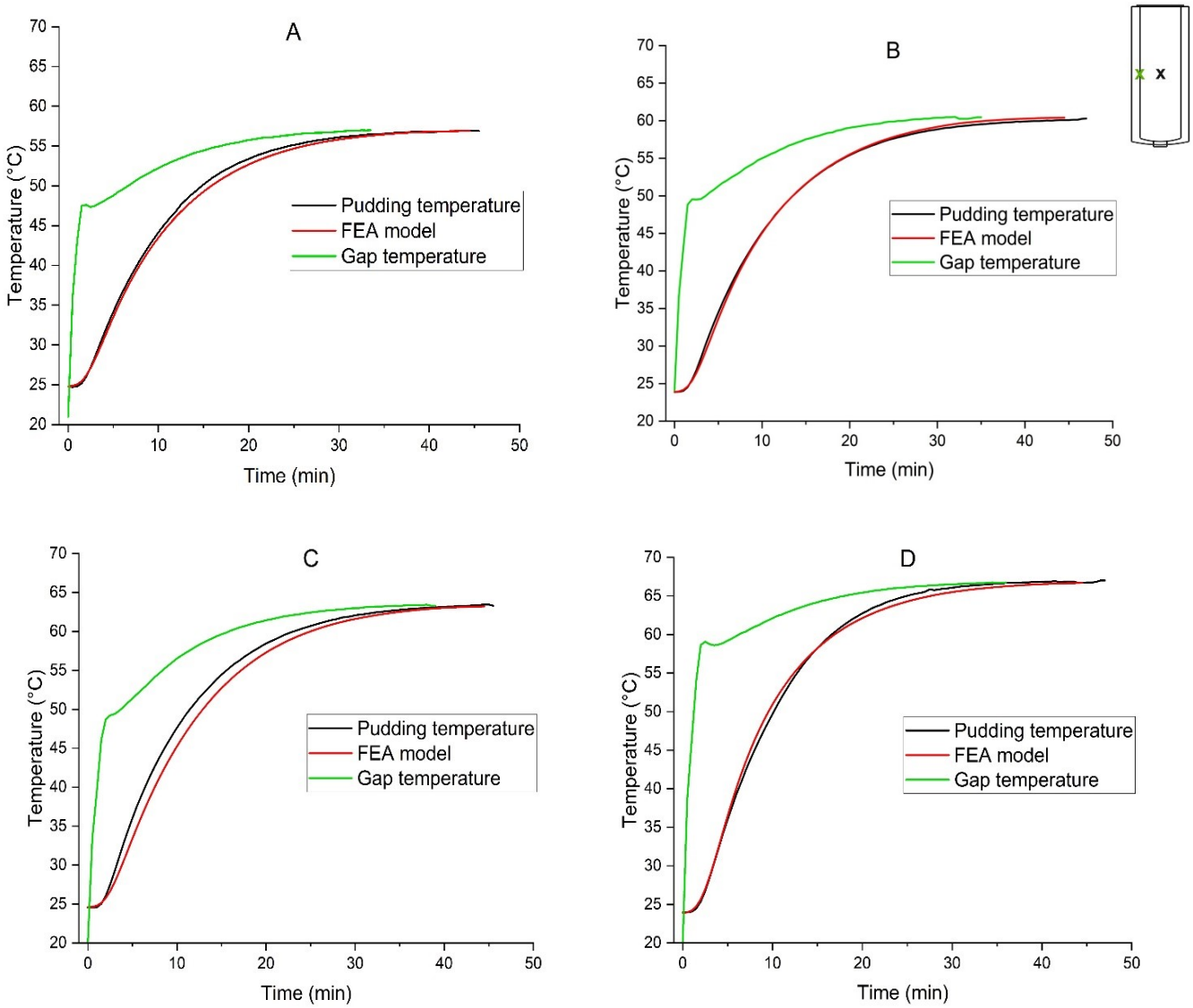

Figure 11. Time-temperature graphs comparing experimentally measured interior temperatures (pudding) and exterior temperatures (gap) with the FEA simulated temperature results for profiles A (55/56.9°C), B (58/60.3°C), C (61/63.3°C) and D (64/66.7°C).

Yang and Rao (1998) studied starch gelatinization and compared a thermo-rheological FEA model of 3.5% cornstarch dispersion in a can with an experimental center of a can time-temperature profile. Starch-filled cans were subjected to saturated steam at 121°C until the geometric center temperature was within 1.5°C of 121°C, as measured by type T thermocouple. The FEA modelling was based on a heat transfer in a 2D cylindrical container using a Fluid Dynamics Analysis Program at 10 s intervals. Heat penetration data showed that predicted transient temperatures were overall a good fit with the experimental values. The highest deviation was shown to be 20% during initial heating, which corresponds with the high deviation leading up to come-up time for all temperature profiles in this study.

Kızıltaş et al. (2010) simulated temperature changes of canned in water peas in a 2D axisymmetric analysis. The study measured the temperature in the geometric center of the can (peas) as well as off-center (water) while heated in a vertical retort at 98°C. The comparison showed that simulation overestimated the temperature in the center by approximately 2°C and underestimated the temperature on top and bottom of the can by approximately 5°C. The results from this study displayed a similar pattern, with simulation underestimating the temperature by maximum of 0.9°C, 1.0°C and 2.7°C for profiles A, B and C, and overestimating the temperature for profile D by 1.3°C. The variability of the gap temperature measurements was greater than the interior (pudding) measurements likely due to some variability in how the syringe sat in the heating barrel. The gap between the syringe and barrel was approximately 0.15 cm, which can allow for some movement of the thermocouple relative to the inside wall of the heating barrel. This variability in positioning between replicate tests may be the main cause of the variability in temperature measurements at the gap.

5.3 Contour plots

Fig. 12 shows the contour plots (i.e., heat maps) demonstrating the heating rate of the pudding in the syringe over time. Each contour plot represents a cross-section of the upper half of the syringe cylinder with the origin placed at the midway point along the cylindrical axis (z-axis in the figure). Initial heating started from the outside walls of syringe, moving into the center of the pudding. There was a noticeable visual temperature difference at the 20 min mark for all temperature profiles, indicating a cold spot. The temperature increased first on the outside walls of the syringe, heated down to the center, and finally migrated through to the top of the syringe. There was still uncertainty about the loss of heat through convection at the top, which requires further experiments closer to the rubber stopper to determine more accurate values. Rapid temperature increase is more pronounced in profile D due to higher initial temperature, with the hottest temperature of 66.8°C in the middle of the pudding and the lowest temperature of 49.4°C at the top at 50 min.

Kızıltaş et al. (2010) also showed the temperature contour plots of canned peas at 30 s and 300 s, demonstrating the movement of the slowest heating zone from the center of the can towards the bottom, as natural convection heating was expanding from the top towards the middle of the can, pushing the cold spot downwards. Shafiekhani et al. (2016) modeled the pasteurization of canned apple puree in an aluminum-based container via retort. The results of the predicted (simulated) average temperature values were not significantly (p <0.01) different from experimental temperature values. The study noted that the slowest heating zone expanded when there was less headspace in the container, which can be seen in Fig. 12 with the cold spot located vertically through the cylinder across all temperature profiles.

Overall, numerical modeling is a useful tool to pair with novel technologies like 3DFP. It allows to study a variety of container shapes and products in a less time consuming and costly

way than measuring the temperature changes experimentally, like in a case of heat transfer. Validation of simulation results is important in the initial stages of research, however, once a protocol is established for a certain food medium and pathogen, a system can be designed to predict temperature changes and bacterial inactivation across various scenarios.

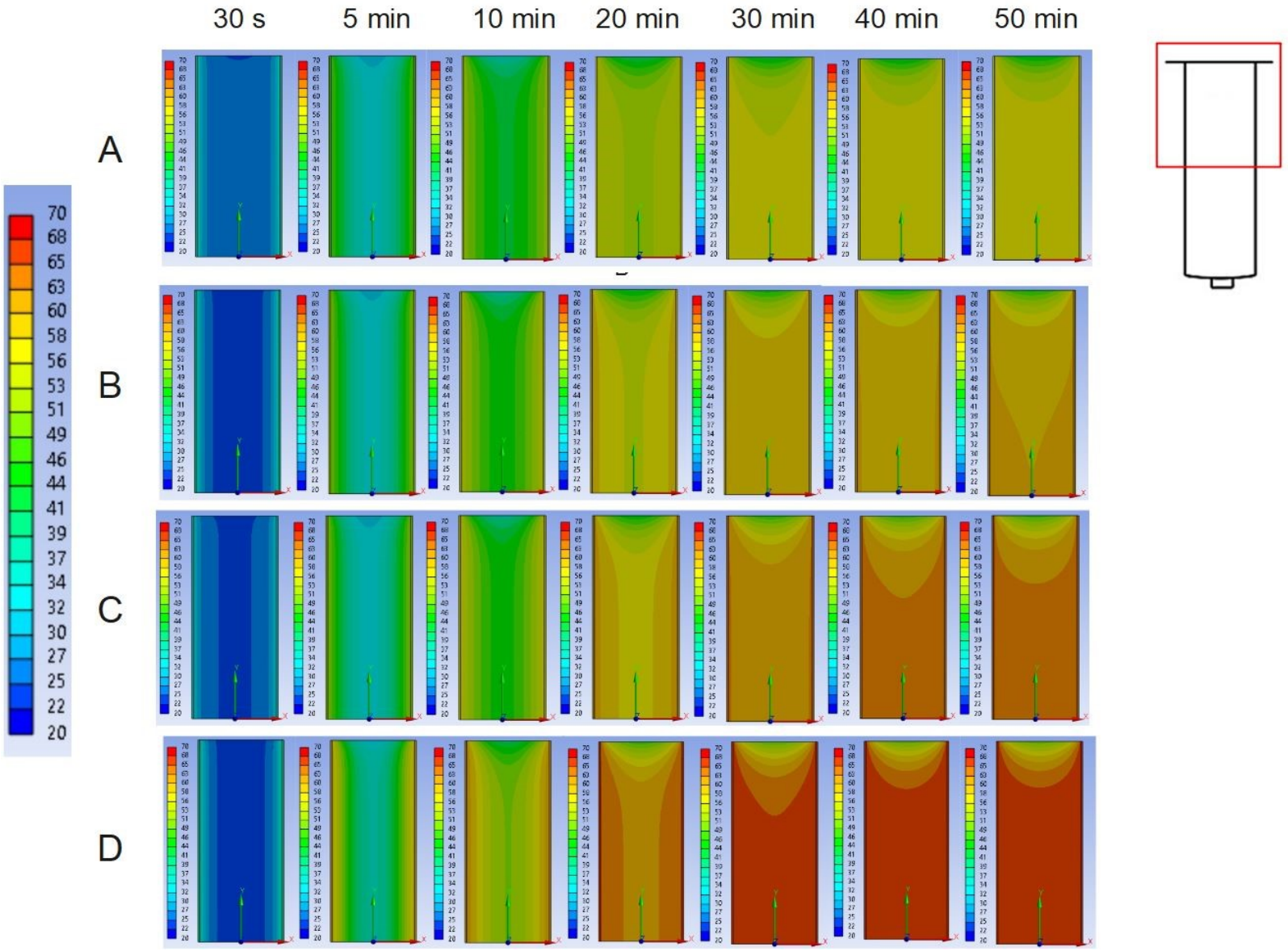

Figure 12. Contour plots of the heating rate of the pudding in the syringe upper half over time increments of 30s, 5 min, 10 min, 20 min, 30 min, 40 min and 50 min for temperature profiles A (55/56.9°C), B (58/60.3°C), C (61/63.3°C) and D (64/66.7°C).

Chapter 6: Conclusions and recommendations

6.1 Summary of key findings

The main objective of this study was to determine the effect of four temperature profiles (A, B, C and D) and four time (10, 20, 30 and 40 min) combinations on *Salmonella* inactivation in a 3DFP high moisture pudding samples. Temperature profiles indicated the set printer temperature and the actual reached temperature, i.e. A was 55°C/56.9°C, B was 58°C/60.3°C, C was 61°C/63.3°C and D was 64°C/66.7°C, respectively.

There is limited research related to microbiological safety of 3D printed foods with most of the studies focusing on printability and qualitative analysis. This study offers an insight into inactivation of heat sensitive strain *S. enterica* serovar Typhimurium via heated extrusion of a commercial RTE pudding in a 3DFP. Significant reductions in Salmonella populations were achieved with 2-4 log at lower temperatures and longer time combinations, as well higher temperatures-shorter time combinations. Up to 7 log reductions were observed for temperature profiles C and D at 40 min treatment time. 10 min treatments time did not affect *Salmonella* population for all temperature profiles, indicating some heat resistance of the strain at lower temperatures. The D_v values were introduced to account for non-isothermal variable printing conditions and were calculated to be 18.18 min, 7.65 min, 4.88 min and 4.93 min for profiles A, B, C and D, respectively. Z_v was determined to be 17.1°C. Temperature profiles C and D had similar D_v values, indicating bacterial heat sensitivity at higher temperatures. Since the quality of food product might be affected at higher temperatures and combinations B-40 and C-30 had the same log reduction values, it might be beneficial to heat the product for a longer period of time at a lower temperature. If higher temperature is chosen, profile C was comparable to D in terms of time needed for 90% reduction of *Salmonella* population. Thermal inactivation of *S. enterica* in

3DFP pudding samples was found to be non-linear, so a better fitting model like Weibull should be used in the future for accurate data fitting. Overall, microbial inactivation results showed that 3DFP with hot extrusion can be used to mitigate pathogens with proper selection of a temperature-time profile.

Finite element analysis (FEA) modeling was used to supplement obtained microbiological data. Since there has been limited use of FEA in 3DFP area, this work demonstrates possible use of numerical model in conjunction with novel technologies for mitigation of pathogens. The simulation results were validated by experimentally obtained temperature change values and were overall a good fit. Gap temperature measurements provided an insight into how the food printer's heating mechanism works. The contour plots demonstrated the position of cold spot inside the pudding and its movement upwards, revealing the need for more accurate measurements of the convection term near the syringe top. Paired with the inactivation results, FEA can be useful for designing a system of pathogen mitigation during the 3DFP process, possibly extending to more pathogens and food products in the future.

6.2 Recommendations for future research

Areas of future research:

1. Accurate measurements of true D and z-values are needed to better understand the thermal destruction of *Salmonella* in an extrusion-based 3DP featuring a heating element. Utilizing a Weibull model can provide a better understanding of thermal inactivation kinetics since the heating process in a 3DFP was non-isothermal.
2. More experimental temperature measurements are required at the top quarter point of the syringe closer to the rubber stopper to investigate more accurate heat loss via conduction.

3. The quality of pudding, as well as other extrudable products, might be impacted at higher temperatures and longer times, therefore, a qualitative analysis is necessary. This is more crucial in the case of foods fortified or encapsulated with vitamins and bioactive compounds. Color change measurements, textural and rheological properties like viscosity and cohesiveness, post-processing stability and vitamin retention are some of the qualitative tests recommended.
4. Other foodborne pathogens need to be studied in conjunction with a variety of extrudable food products to expand the field of microbiological safety in 3DFP.
5. Integrating non-thermal technologies like cold plasma for surface decontamination and sterilization of food printers.

.

References

Angelotti, R., Foter, M. J., & Lewis, K. H. (1961). Time-temperature effects on Salmonellae and Staphylococci in foods. III. Thermal death time studies. *Applied Microbiology*, *9*, 308–315.

Antunović, B., Kovaček, I., Gvozdanović, K., Grčević, M., Gantner, V., Poljak, V., Ostović, M., Pavičić, Ž., & Ahmetović, N. (2018). Influence of milk product type and its initial contamination on the efficiency of different methods for detection of *Salmonella Enteritidis, Listeria monocytogenes* and *Escherichia coli* O157:H7: Utjecaj vrste mliječnih proizvoda i početne kontaminacije na učinkovitost različitih metoda dokazivanja bakterija *Salmonella Enteritidis, Listeria monocytogenes* i *Escherichia coli* O157:H7. *Dairy / Mljekarstvo*, *68*(1), 3–11. https://doi.org/10.15567/mljekarstvo.2018.0101

Anukiruthika, T., Moses, J. A., & Anandharamakrishnan, C. (2020). 3D printing of egg yolk and white with rice flour blends. *Journal of Food Engineering*, *265*. https://doi.org/10.1016/j.jfoodeng.2019.109691

Baiano, A. (2022). 3D Printed Foods: A Comprehensive Review on Technologies, Nutritional Value, Safety, Consumer Attitude, Regulatory Framework, and Economic and Sustainability Issues. *Food Reviews International*, *38*(5), 986–1016. https://doi.org/10.1080/87559129.2020.1762091

Barbosa-Cánovas, G. V., Fontana, A. J., Jr., Schmidt, S. J., & Labuza, T. P. (2020). *Water Activity in Foods: Fundamentals and Applications*. John Wiley & Sons, Incorporated. http://ebookcentral.proquest.com/lib/ualberta/detail.action?docID=6198566

Bareen, M. A., Sahu, J. K., Prakash, S., Bhandari, B., & Naik, S. (2023). A novel approach to produce ready-to-eat sweetmeats with variable textures using 3D printing. *Journal of Food Engineering*, *344*, 111410. https://doi.org/10.1016/j.jfoodeng.2023.111410

Berk, Z. (2008). *Food Process Engineering and Technology*. Elsevier Science & Technology. http://ebookcentral.proquest.com/lib/ualberta/detail.action?docID=369462

Beuchat, L. R., & Mann, D. A. (2010). Survival and Growth of *Salmonella* in High-Moisture Pecan Nutmeats, In-Shell Pecans, Inedible Nut Components, and Orchard Soil. *Journal of Food Protection*, *73*(11), 1975–1985. https://doi.org/10.4315/0362-028X-73.11.1975

Bhavikatti, S. S. (2005). *Finite element analysis. [Electronic resource]* (Concordia University of Edmonton - Online Resources Internet Access). New Age International (P) Ltd., Publishers.

Choi, W., Kim, S., Park, S., Ahn, J., & Kang, D. (2020). Numerical analysis of rectangular type batch ohmic heater to identify the cold point. *Food Science & Nutrition*, *8*(1), 648–658. https://doi.org/10.1002/fsn3.1353

Derossi, A., Caporizzi, R., Azzollini, D., & Severini, C. (2018). Application of 3D printing for customized food. A case on the development of a fruit-based snack for children. *Journal of Food Engineering*, *220*, 65–75. https://doi.org/10.1016/j.jfoodeng.2017.05.015

Dhaliwal, H. K., Gänzle, M., & Roopesh, M. S. (2021). Influence of drying conditions, food composition, and water activity on the thermal resistance of *Salmonella enterica*. *Food Research International*, *147*. https://doi.org/10.1016/j.foodres.2021.110548

Enfield, R. E., Pandya, J. K., Lu, J., McClements, D. J., & Kinchla, A. J. (2023). The future of 3D food printing: Opportunities for space applications. *Critical Reviews in Food Science and Nutrition*, *63*(29), 10079–10092. https://doi.org/10.1080/10408398.2022.2077299

Fabbri, A., & Cevoli, C. (2015). 2D water transfer finite elements model of salami drying, based on real slice image and simplified geometry. *Journal of Food Engineering*, *158*, 73–79. https://doi.org/10.1016/j.jfoodeng.2015.03.005

Fabrega, A., & Vila, J. (2013). *Salmonella enterica* Serovar Typhimurium Skills To Succeed in the Host: Virulence and Regulation. *Clinical Microbiology Reviews*, *26*(2), 308–341. https://doi.org/10.1128/CMR.00066-12

Fadiji, T., Coetzee, C. J., Berry, T. M., Ambaw, A., & Opara, U. L. (2018). The efficacy of finite element analysis (FEA) as a design tool for food packaging: A review. *Biosystems Engineering*, *174*, 20–40. https://doi.org/10.1016/j.biosystemseng.2018.06.015

Featherstone, S. (2015). *A Complete Course in Canning and Related Processes* (University of Alberta - Internet Internet Access; 281st ed.). Woodhead Publishing.

Ford, L., Moffatt, C. R. M., Fearnley, E., Polkinghorne, B. G., Franklin, N., Glass, K., Kirk, M. D., Miller, M., Gregory, J., Sloan-Gardner, T. S., Bell, R., & Williamson, D. A. (2018). The Epidemiology of *Salmonella enterica* Outbreaks in Australia, 2001–2016. *Frontiers in Sustainable Food Systems*, *2*. https://doi.org/10.3389/fsufs.2018.00086

Gibson, B. (1973). The Effect of High Sugar Concentrations on the Heat Resistance of Vegetative Micro-organisms. *Journal of Applied Bacteriology*, *36*(3), 365–376. https://doi.org/10.1111/j.1365-2672.1973.tb04118.x

Godoi, F. C. (2019). *Fundamentals of 3D food printing and applications* (MacEwan University - Internet Internet Access). Elsevier Ltd.

Godoi, F. C., Bhandari, B. R., Prakash, S., & Zhang, M. (2019). Chapter 1—An Introduction to the Principles of 3D Food Printing. In F. C. Godoi, B. R. Bhandari, S. Prakash, & M. Zhang (Eds.), *Fundamentals of 3D Food Printing and Applications* (pp. 1–18). Academic Press. https://doi.org/10.1016/B978-0-12-814564-7.00001-8

Government of Canada, C. F. I. A. (2012, November 14). *Equipment—General Principles of Food Hygiene, Composition and Labelling*. https://inspection.canada.ca/food-safety-for-industry/archived-food-guidance/non-federally-registered/safe-food-production/general-principles/eng/1352919343654/1352920880237?chap=3

Hamilton, A. N., & Gibson, K. E. (2023). Transfer rates of *Salmonella* Typhimurium, *Listeria monocytogenes*, and a human norovirus surrogate impacted by macronutrient composition of food inks in 3D food printing systems. *Food Microbiology*, *113*, N.PAG-N.PAG. https://doi.org/10.1016/j.fm.2023.104268

He, Y., Guo, D., Zhang, W., Yang, J., & Tortorello, M. l. (2011). Survival and heat resistance of *Salmonella enterica* and *Escherichia coli* O157:H7 in peanut butter. *Applied and Environmental Microbiology*, *77*(23), 8434–8438. https://doi.org/10.1128/AEM.06270-11

Jagtap, S., Salonitis, K., Bader, F., Trollman, H., Garcia-Garcia, G., & Fadiji, T. (2021). Food Logistics 4.0: Opportunities and Challenges. *Logistics*, *5*(1). https://doi.org/10.3390/logistics5010002

Kern, C., Hinrichs, J., & Weiss, J. (2018). Additive layer manufacturing of semi-hard model cheese: Effect of calcium levels on thermo-rheological properties and shear behavior. *Journal of Food Engineering*, *235*, 89–97. https://doi.org/10.1016/j.jfoodeng.2018.04.029

Kızıltaş, S., Erdoğdu, F., & Koray Palazoğlu, T. (2010). Simulation of heat transfer for solid–liquid food mixtures in cans and model validation under pasteurization conditions. *Journal of Food Engineering*, *97*(4), 449–456. https://doi.org/10.1016/j.jfoodeng.2009.10.042

Korver, D., & McMullen, L. (2017). Chapter 4—Egg Production Systems and *Salmonella* in Canada. In S. C. Ricke & R. K. Gast (Eds.), *Producing Safe Eggs* (pp. 59–69). Academic Press. https://doi.org/10.1016/B978-0-12-802582-6.00004-5

Kumar, L., & Prakash, O. (2023). Development of FE modeling for hybrid greenhouse dryer for potato chips drying. *Journal of Food Science*, *88*(5), 1800–1815. https://doi.org/10.1111/1750-3841.16525

Lanaro, M., Forrestal, D. P., Scheurer, S., Slinger, D. J., Liao, S., Powell, S. K., & Woodruff, M. A. (2017). 3D printing complex chocolate objects: Platform design, optimization and evaluation. *Journal of Food Engineering*, *215*, 13–22. https://doi.org/10.1016/j.jfoodeng.2017.06.029

Le Tohic, C., O'Sullivan, J. J., Drapala, K. P., Chartrin, V., Chan, T., Kerry, J. P., Kelly, A. l., & Morrison, A. P. (2018). Effect of 3D printing on the structure and textural properties of processed cheese. *Journal of Food Engineering*, *220*, 56–64. https://doi.org/10.1016/j.jfoodeng.2017.02.003

Li, H., Koontz, J., Megalis, C., Fleischman, G., Tortorello, M. l., Fu, X., Bima, Y., & Yang, F. (2014). Effect of the local microenvironment on survival and thermal inactivation of *Salmonella* in low- and intermediate-moisture multi-ingredient foods. *Journal of Food Protection*, *77*(1), 67–74. https://doi.org/10.4315/0362-028X.JFP-13-277

Lille, M., Nurmela, A., Nordlund, E., Metsä-Kortelainen, S., & Sozer, N. (2018). Applicability of protein and fiber-rich food materials in extrusion-based 3D printing. *Journal of Food Engineering*, *220*, 20–27. https://doi.org/10.1016/j.jfoodeng.2017.04.034

Lipton, J., Arnold, D., Nigl, F., Lopez, N., Cohen, D., Norén, N., & Lipson, H. (2010). *Multi-material food printing with complex internal structure suitable for conventional post-processing," in 21st Solid Freeform Fabrication Symposium. The University of Texas at*.

Lipton, J., Cutler, M., Nigi, F., Cohen, D., & Lipson, H. (2015). Additive manufacturing for the food industry. *Trends in Food Science & Technology*, *43*(1), 114–123. https://doi.org/10.1016/j.tifs.2015.02.004

Liu, L., Meng, Y., Dai, X., Chen, K., & Zhu, Y. (2019). 3D Printing Complex Egg White Protein Objects: Properties and Optimization. *Food and Bioprocess Technology: An International Journal*, *12*(2), 267–279. https://doi.org/10.1007/s11947-018-2209-z

Liu, Y., Liu, D., Wei, G., Ma, Y., Zhou, P., & Bhandari, B. (2018). 3D printed milk protein food simulant: Improving the printing performance of milk protein concentration by incorporating whey protein isolate. *Innovative Food Science and Emerging Technologies*, *49*, 116–126. https://doi.org/10.1016/j.ifset.2018.07.018

Liu, Z., Zhang, M., Bhandari, B., & Wang, Y. (2017). 3D printing: Printing precision and application in food sector. *Trends in Food Science & Technology*, *69*, 83–94. https://doi.org/10.1016/j.tifs.2017.08.018

Liu, Z., Zhang, M., & Yang, C.-H. (2018). Dual extrusion 3D printing of mashed potatoes/strawberry juice gel. *LWT - Food Science and Technology*, *96*, 589–596. https://doi.org/10.1016/j.lwt.2018.06.014

Madenci, E. (2015). *The finite element method and applications in engineering using ANSYS®* (University of Alberta - Online Resources Internet Access; Second edition.). Springer.

Mantihal, S., Prakash, S., Godoi, F., & Bhandari, B. (2019). Effect of additives on thermal, rheological and tribological properties of 3D printed dark chocolate. *Food Research International*, *119*, 161–169. https://doi.org/10.1016/j.foodres.2019.01.056

Márquez-González, M., Velásquez-Moreno, C. G., García-Lira, A. G., & Osorio, L. F. (2022). Thermal Inactivation of *Salmonella enterica* and *Listeria monocytogenes* in Quesillo Manufactured from Raw Milk. *International Journal of Food Science*, *2022*. https://doi.org/10.1155/2022/2507867

Martinez-Monzo, J., Cardenas, J., & Garcia-Segovia, P. (2019). Effect of Temperature on 3D Printing of Commercial Potato Puree. *Food Biophysics*, *14*(3), 225–234. https://doi.org/10.1007/s11483-019-09576-0

Mashhood, M., Peters, B., Zilian, A., Baroli, D., & Wyart, E. (2023). Developing the AM G-code based thermomechanical finite element platform for the analysis of thermal

deformation and stress in metal additive manufacturing process. *Journal of Mechanical Science and Technology*, *37*(3), 1103–1112. https://doi.org/10.1007/s12206-022-2106-2

McHugh, T., & Thai. (2020, January 1). *Canning Clarified*. Institute of Food Technologists (IFT). https://www.ift.org/news-and-publications/food-technology-magazine/issues/2020/january/columns/canning-clarified

Mercer, R. G., Walker, B. D., Yang, X., McMullen, L. M., & Gänzle, M. G. (2017). The locus of heat resistance (LHR) mediates heat resistance in *Salmonella enterica, Escherichia coli* and *Enterobacter cloacae*. *Food Microbiology*, *64*, 96–103. https://doi.org/10.1016/j.fm.2016.12.018

Morton, V. K., Viswanathan, M., Hexemer, A., Kearney, A., Coleman, S., Chau, K., & Orr, A. (2019). Outbreaks of *Salmonella* illness associated with frozen raw breaded chicken products in Canada, 2015–2019. *Epidemiology and Infection*, *147*. https://doi.org/10.1017/S0950268819001432

Moura-Alves, M., Machado, C., Silva, J. A., & Saraiva, C. (2020). Determination of D and z values for *Salmonella* Typhimurium inoculated in an egg-based pastry. *Brazilian Journal of Food Technology*, *23*. https://doi.org/10.1590/1981-6723.12219

Muro-Fraguas, I., Sainz-García, A., Múgica-Vidal, R., Sainz-García, E., González-Marcos, A., Alba-Elías, F., Fernández Gómez, P., López, M., González-Raurich, M., Prieto, M., Alvarez-Ordóñez, A., López, M., Toledano, P., & Sáenz, Y. (2020). Atmospheric pressure cold plasma anti-biofilm coatings for 3D printed food tools. *Innovative Food Science and Emerging Technologies*, *64*. https://doi.org/10.1016/j.ifset.2020.102404

Nijdam, J. J., Agarwal, D., & Schon, B. S. (2021). Assessment of a novel window of dimensional stability for screening food inks for 3D printing. *Journal of Food Engineering*, *292*, 110349. https://doi.org/10.1016/j.jfoodeng.2020.110349

Osasah, V., Whitfield, Y., Adams, J., Danish, A., Mather, R., & Aloosh, M. (2023). An Outbreak of *Salmonella* Typhimurium Infections Linked to Ready-To-Eat Tofu in Multiple Health Districts—Ontario, Canada, May-July 2021. *MMWR: Morbidity & Mortality Weekly Report*, *72*(32), 855–858. https://doi.org/10.15585/mmwr.mm7232a1

Ouldyerou, A., Aminallah, L., Merdji, A., Mehboob, A., & Mehboob, H. (2023). Finite element analyses of porous dental implant designs based on 3D printing concept to evaluate biomechanical behaviors of healthy and osteoporotic bones. *Mechanics of Advanced Materials and Structures*, *30*(11), 2328–2340. https://doi.org/10.1080/15376494.2022.2053908

Outbreaks Involving Salmonella | CDC. (2022, May 21). https://www.cdc.gov/salmonella/outbreaks.html

Pandit, R. B., & Prasad, S. (2003). Finite element analysis of microwave heating of potato–transient temperature profiles. *Journal of Food Engineering*, *60*(2), 193–202. https://doi.org/10.1016/S0260-8774(03)00040-2

Papas, N., Tsongas, K., Karolidis, D., & Tzetzis, D. (2023). The integration of 3D technologies and finite element analysis (FEA) for the restoration of an ancient terra sigillata plate. *Digital Applications in Archaeology and Cultural Heritage*, *28*, e00260. https://doi.org/10.1016/j.daach.2023.e00260

Park, J. W., Lee, S. H., Kim, H. W., & Park, H. J. (2023). Application of extrusion-based 3D food printing to regulate marbling patterns of restructured beef steak. *Meat Science*, *202*. https://doi.org/10.1016/j.meatsci.2023.109203

Porto-Fett, A. C. S., Shoyer, B. A., Shane, L. E., Osoria, M., Henry, E., Jung, Y., & Luchansky, J. B. (2019). Thermal Inactivation of *Salmonella* in Pâté Made from Chicken Liver. *Journal of Food Protection*, *82*(6), 980–987. https://doi.org/10.4315/0362-028X.JFP-18-423

Sampson, G. L., Ruelle, S. B., Phan, L., Williams-Hill, D., & Hellberg, R. S. (2023). Effectiveness of selected pre-enrichment broths for the detection of *Salmonella* spp. In meat analogs. *Food Control*, *143*. https://doi.org/10.1016/j.foodcont.2022.109282

Santos, M. V., Zaritzky, N., & Califano, A. (2008). Modeling heat transfer and inactivation of *Escherichia coli* O157:H7 in precooked meat products in Argentina using the finite element method. *Meat Science*, *79*(3), 595–602. https://doi.org/10.1016/j.meatsci.2007.12.014

Severini, C., Derossi, A., Ricci, I., Caporizzi, R., & Fiore, A. (2018). Printing a blend of fruit and vegetables. New advances on critical variables and shelf life of 3D edible objects. *Journal of Food Engineering*, *220*, 89–100. https://doi.org/10.1016/j.jfoodeng.2017.08.025

Shafiekhani, S., Zamindar, N., Hojatoleslami, M., & Toghraie, D. (2016). Numerical simulation of transient temperature profiles for canned apple puree in semi-rigid aluminum-based

packaging during pasteurization. *Journal of Food Science and Technology*, *53*(6), 2770–2778. https://doi.org/10.1007/s13197-016-2249-1

Silva, F. M., & Evelyn, E. (2023). Pasteurization of Food and Beverages by High Pressure Processing (HPP) at Room Temperature: Inactivation of *Staphylococcus aureus, Escherichia coli, Listeria monocytogenes, Salmonella*, and Other Microbial Pathogens. *Applied Sciences*, *13*(2), Article 2. https://doi.org/10.3390/app13021193

Singh, R. P., & Heldman, D. R. (1984). *Introduction to Food Engineering* (University of Alberta - Online Resources Internet Access). Academic Press.

Sun, J., Zhou, W., Huang, D., Fuh, J. Y. H., & Hong, G. S. (2015). An Overview of 3D Printing Technologies for Food Fabrication. *Food and Bioprocess Technology*, *8*(8), 1605–1615. https://doi.org/10.1007/s11947-015-1528-6

Sun, J., Zhou, W., Huang, D., Yan, L., & Lin, L.-Y. (2018). Extrusion-based food printing for digitalized food design and nutrition control. *Journal of Food Engineering*, *220*, 1–11. https://doi.org/10.1016/j.jfoodeng.2017.02.028

Sundarsingh, A., Zhang, M., Mujumdar, A. S., & Li, J. (2023). Research Progress in Printing Formulation for 3D Printing of Healthy Future Foods. *Food and Bioprocess Technology: An International Journal*, 1–32. https://doi.org/10.1007/s11947-023-03265-0

Tahmasebinia, F., Jabbari, A. A., & Skrzypkowski, K. (2023). The Application of Finite Element Simulation and 3D Printing in Structural Design within Construction Industry 4.0. *Applied Sciences*, *13*(6), Article 6. https://doi.org/10.3390/app13063929

Tobi Fadiji, Seyed-Hassan Miraei Ashtiani, Daniel I. Onwude, Zhiguo Li, & Umezuruike Linus Opara. (2021). Finite Element Method for Freezing and Thawing Industrial Food Processes. *Foods*, *10*(869), 869–869. https://doi.org/10.3390/foods10040869

Verma, V. K., Kamble, S. S., Ganapathy, L., Belhadi, A., & Gupta, S. (2022). 3D Printing for sustainable food supply chains: Modelling the implementation barriers. *International Journal of Logistics Research and Applications*, *0*(0), 1–27. https://doi.org/10.1080/13675567.2022.2037125

Wang, L., Zhang, M., Bhandari, B., & Yang, C. (2018). Investigation on fish surimi gel as promising food material for 3D printing. *Journal of Food Engineering*, *220*, 101–108. https://doi.org/10.1016/j.jfoodeng.2017.02.029

Xu, J., Tang, J., Jin, Y., Yang, R., Sablani, S. S., Song, J., & Zhu, M. J. (2019). High temperature water activity as a key factor influencing survival of *Salmonella* Enteritidis PT30 in thermal processing. *Food Control*, *98*, 520–528. https://doi.org/10.1016/j.foodcont.2018.11.054

Yang, F., Zhang, M., & Bhandari, B. (2017). Recent development in 3D food printing. *Critical Reviews in Food Science and Nutrition*, *57*(14), 3145–3153. https://doi.org/10.1080/10408398.2015.1094732

Yang, W. H., & Rao, M. A. (1998). Transient natural convection heat transfer to starch dispersion in a cylindrical container: Numerical solution and experiment. *Journal of Food Engineering*, *36*(4), 395–415. https://doi.org/10.1016/S0260-8774(98)00069-7

Yazicioglu, N., Sumnu, G., & Sahin, S. (2021). Heat and mass transfer modeling of microwave infrared cooking of zucchini based on Lambert law. *Journal of Food Process Engineering*, e13895. https://doi.org/10.1111/jfpe.13895

Ye, R. (2023, April 23). *Additive Manufacturing vs Subtractive Manufacturing: In-depth Comparison & Differences*. Rapid Prototyping & Low Volume Production. https://www.3erp.com/blog/additive-vs-subtractive-manufacturing/

Zhang, J. Y., Pandya, J. K., McClements, D. J., Lu, J., & Kinchla, A. J. (2022). Advancements in 3D food printing: A comprehensive overview of properties and opportunities. *Critical Reviews in Food Science & Nutrition*, *62*(17), 4752–4768. https://doi.org/10.1080/10408398.2021.1878103

Zhang, L., Lou, Y., & Schutyser, M. A. (2018). 3D printing of cereal-based food structures containing probiotics. *Food Structure: Netherlands*, *18*, 14–22. https://doi.org/10.1016/j.foostr.2018.10.002

Zhou, L., Puri, V. M., Anantheswaran, R. C., & Yeh, G. (1995). Finite element modeling of heat and mass transfer in food materials during microwave heating—Model development and validation. *Journal of Food Engineering*, *25*(4), 509–529.